

Supporting Information (SI)

A Narrow-Bandgap Non-Fullerene Acceptor Constructed by S,N-Heteroacene Up to a Dodecamer in Size

Jiixin Guo^{†,[a]}, Xinyuan Jia^{†,[a]}, Xiangjian Cao^[a], Tengfei He^[a], Huazhe Liang^[a], Wendi Shi^[a], Zheng Xu^[a], Ruohan Wang^[a], Yaxiao Guo^{*,[b]}, Zhaoyang Yao^{*,[a]}, Xiangjian Wan^[a], Guankui Long^[c], Chenxi Li^[a], Yongsheng Chen^{*,[a]}

^[a]State Key Laboratory and Institute of Elemento-Organic Chemistry, The Centre of Nanoscale Science and Technology and Key Laboratory of Functional Polymer Materials, Renewable Energy Conversion and Storage Center (RECAST), College of Chemistry, Nankai University, Tianjin 300071, China.

^[b]State Key Laboratory of Separation Membranes and Membrane Processes, School of Chemistry, Tiangong University, Tianjin 300387, China.

^[c]School of Materials Science and Engineering, National Institute for Advanced Materials, Renewable Energy Conversion and Storage Center (RECAST), Nankai University, 300350, Tianjin, China.

[†]These authors contributed equally: Jiixin Guo and Xinyuan Jia.

Corresponding E-mails: yschen99@nankai.edu.cn (Y.C.); zyao@nankai.edu.cn (Z.Y.); yaxiaoguo@tiangong.edu.cn.

Contents

1. Materials and Methods.....	2
2. Synthesis of JX1 and JX2.....	6
2.1 Synthesis of JX1.....	6
2.2 Synthesis of JX2.....	10
3. Figures (S1-S31).....	14
3.1 Photophysical properties of JX1 and JX2.....	14
3.2. Photovoltaic device performance.....	15
3.3. Morphology analysis.....	19
3.3. E_{loss} analysis.....	21
4. Note S1.....	35
5. Tables S1-S7.....	37
6. References.....	42

1. Materials and Methods.

Materials.

All the starting materials and common reagents were purchased from commercial suppliers and used without further purification unless indicated otherwise. Polymeric donor PCE10 were purchased from Solarmer Material (Beijing) Inc. Compounds 2,5-bis(trimethylstannyl)thieno[3,2-b]thiophene was synthesized according to previous report methods¹. The overall synthesis route and detailed synthesized procedures of JX1 and JX2 the corresponding characterizations were displayed in “Synthesis of JX1 and JX2” below.

Methods.

Computational methods in this work. All the alkyl chains were replaced with methyl groups (-CH₃) to reduce the computational requirements. The structures were subsequently optimized with Density Functional Theory (DFT) in vacuum within the Gaussian 16 software. The structure optimization, frequency analysis and energy level of frontier molecular orbital were obtained at the Becke three-parameter Lee-Yang-Parr (B3LYP)² hybrid functional with the 6-31G(d) basis set³.

UV-visible (UV-*Vis*) absorption. UV-*Vis* spectra were obtained by a Cary 5000 UV-*Vis* spectrophotometer. The diluted solutions of JX1 and JX2 were kept at a low concentration of 10⁻⁵ M.

The nuclear magnetic resonance (NMR) spectra and High-Resolution Mass Spectra (HRMS). The ¹H/¹³C nuclear magnetic resonance (¹H/¹³C NMR) spectra of all compounds were obtained from a Bruker AV400 Spectrometer. The High-Resolution

Mass Spectra (HRMS) were recorded by Solarix scimax MRMS with high-resolution matrix-assisted laser desorption/ionization (HR-MALDI).

Cyclic voltammetry (CV). The CV experiments were performed with a LK98B II Microcomputer-based Electrochemical Analyzer. All measurements were conducted at room temperature with a three-electrode configuration. Among them, a glassy carbon electrode was employed as the working electrode, a saturated calomel electrode (SCE) was used as the reference electrode, and a Pt wire was used as the counter electrode. Tetrabutyl ammonium phosphorus hexafluoride ($n\text{-Bu}_4\text{NPF}_6$, 0.1 M) in acetonitrile was employed as the supporting electrolyte, and the scan rate was kept at 100 mV s^{-1} . Electrochemically reversible ferrocene was employed as internal reference. The HOMO and LUMO energy levels were calculated from the onset oxidation and the onset reduction potentials, respectively, by following the equation $E_{\text{HOMO}} = -(4.80 + E_{\text{ox}}^{\text{onset}})\text{ eV}$, $E_{\text{LUMO}} = -(4.80 + E_{\text{re}}^{\text{onset}})\text{ eV}$.

Atomic force microscopy (AFM). The AFM images were performed using in tapping mode on a Bruker Dimension Icon atomic force microscope.

Grazing incidence wide angle X-ray scattering (GIWAXS). The GIWAXS samples were deposited on Si substrates by use of the same preparation conditions with devices and were carried out at XEUSS SAXS/WAXS equipment.

Photoluminescence (PL). The PL measurements were conducted by using FLS1000 equipment. The emission spectra and PLQY of JX1 and JX2 were obtained using the same setup used for recording electroluminescence spectra excited by an 825 nm wavelength provided by Xenon lamp (Detector for NIR 5509 PMT, 600-1700 nm).

EQE_{EL}. For the EQE_{EL} measurements, a digital source meter (Keithley 2400) was employed to inject electric current into the solar cells, and the emitted photons were collected by a Si diode (Hamamatsu s1337-1010BQ) and indicated by a picoammeter (Keithley 6482).

Highly sensitive EQE (sEQE). sEQE measurements were conducted by using a measurement system containing a halogen lamp light source (LSH-75, Newport), a monochromator (CS260-RG-3-MC-A, Newport), a current amplifier, a chopper and a phase-locked amplifier (SR830, Newport). The overtone signals from the monochromator were blocked by a group of long pass filters (1100 nm, 900 nm, 600 nm).

Device fabrication and measurement. The device structure was ITO/PEDOT:PSS/Active layer/PNDIT-F3N/Ag. ITO coated glass substrates were cleaned with detergent water, deionized water, acetone and isopropyl alcohol in an ultrasonic bath sequentially for 15 mins. Before use, the cleaned ITO substrates were treated with UV exposure for 15 mins in a UV-ozone chamber. A thin layer of PEDOT:PSS (CLEVIOS P VP. AI 4083) was first spin-coated on the substrates at 4300 rpm and baked at 160 °C for 15 mins under ambient conditions. The substrates were then transferred into a nitrogen-filled glove box. Chloroform was chosen as the solvent, and 1,8-diiodooctane (DIO) was chosen as the additive (0.35%, v/v). The concentration of donor is 6 mg/mL, and the weight ratio of PCE10:NFA (PCE10:JX1 and PCE10:JX2) is 1:1.4. The solution was stirred 4 hours for intensive mixing in a nitrogen-filled glove box. The blend solution was spin-cast on the top of PEDOT:PSS layer at 2000 rpm for 30 s. After spin-coating, the blend films were annealed at 90 °C for 5 mins. Then PNDIT-F3N as the electron transporting layer was spin-coated on the

active layer by 3000 rpm from methyl alcohol solution (1 mg/mL). Finally, a layer of Ag with thickness of 150 nm was deposited under 2×10^{-6} Pa. The current density-voltage (J - V) curves of photovoltaic devices were recorded by a Keithley 2400 source-measure unit. The photocurrent was measured under the simulated illumination of 100 mW cm⁻² with AM 1.5 G using a Enli SS-F5-3A solar simulator, which was calibrated by a standard Si solar cell (made by Enli Technology Co., Ltd., Taiwan, and calibrated report can be traced to NREL). Device area is approximately 4 mm². A mask with 2.56 mm² area was used to measure the J - V characteristics. EQE were measured using an Enlitech QE-R EQE system equipped with a standard Si diode in air.

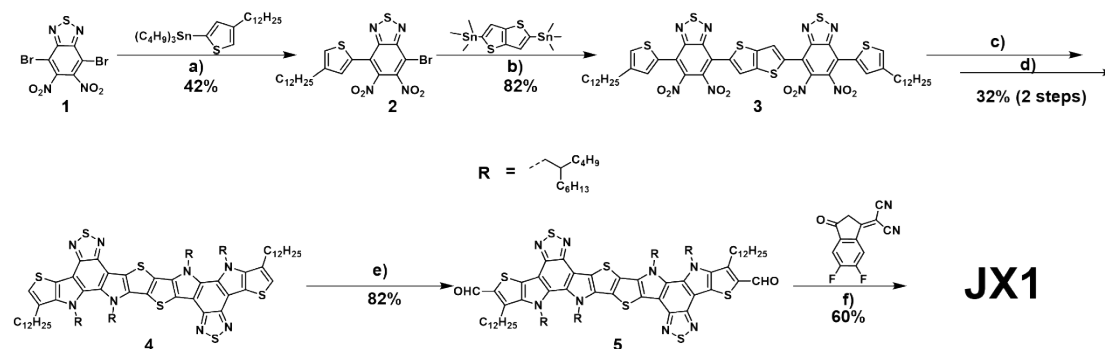
Space-charge-limited current (SCLC) measurement. The SCLC method was used to measure the hole and electron mobilities, by using a diode configuration of ITO/PEDOT:PSS/active layer/MoO₃/Ag for hole and ITO/ZnO/PFN-Br/active layer/PNDIT-F3N/Ag for electron. The dark current density curves were recorded with a bias voltage in the range of 0–8 V. The mobilities were estimated by taking current-voltage curves and fitting the results based on the equation listed below:

$$J = \frac{9\varepsilon_0\varepsilon_r\mu V^2}{8L^3}$$

where J is the current density, ε_0 is the vacuum permittivity, ε_r is the relative dielectric constant, μ is the mobility, and L is the film thickness. V ($=V_{\text{app}} - V_{\text{bi}}$) is the internal voltage in the device, where V_{app} is the applied voltage to the device and V_{bi} is the built-in voltage due to the relative work function difference of the two electrodes.

2. Synthesis of JX1 and JX2.

2.1 Synthesis of JX1



Scheme S1. The overall synthetic route to JX1. Reagents and conditions: a) Pd₂(dba)₃, P(*o*-tolyl)₃, toluene, 60 °C, 2 days; b) Pd₂(dba)₃, P(*o*-tolyl)₃, toluene, reflux, overnight; c) PPh₃, *o*-DCB, reflux, 12 h; d) NaOH, DMF, 5-(Iodomethyl)undecane, 90 °C, 3 days; e) POCl₃, DMF, ClCH₂CH₂Cl, reflux, 12 h; f) 2-(6,7-difluoro-3-oxo-2,3-dihydro-1H-cyclopenta[*b*] naphthalen-1-ylidene) malononitrile, pyridine, CHCl₃, reflux, 12 h.

Synthesis of compound 2. Under the protection of argon, compound 1 (5.0 g, 13.02 mmol), tributyl(4-dodecylthiophen-2-yl)stannane (5.0 g, 9.11 mmol), Pd₂(dba)₃ (476 mg, 0.52 mmol), P(*o*-tolyl)₃ (632 mg, 2.08 mmol) were dissolved in 50 mL of dry toluene and stirred at 60 °C for 2 days. The reaction mixture was allowed to cool to room temperature and then concentrated under reduced pressure. The crude product was chromatographically purified on a silica gel column eluting with dichloromethane/petroleum ether (1/5, v/v) as the eluent to afford compound 2 as a red solid (3.0 g, 42.0% yield). ¹H NMR (400 MHz, CDCl₃) δ 7.28 (d, *J* = 6.9 Hz, 2H), 2.61 (t, *J* = 7.7 Hz, 2H), 1.60 (m, 2H), 1.39 – 1.11 (m, 20H), 0.82 (m, 3H). ¹³C NMR (101 MHz, CDCl₃) δ 152.27, 151.21, 144.95, 144.64, 141.28, 132.61, 128.65, 127.03, 122.82, 108.22, 32.01, 30.42, 30.27, 29.77, 29.74, 29.68, 29.52, 29.45, 29.30, 26.85, 22.78, 14.23.

Synthesis of compound 3. Under the protection of argon, compound 2 (2.0 g, 3.6 mmol), 2,5-bis(trimethylstannyl)thieno[3,2-b]thiophene (763 mg, 1.6 mmol), Pd₂(dba)₃ (130 mg, 0.144 mmol), P(*o*-tolyl)₃ (169 mg, 0.6 mmol) were dissolved in 30 mL of dry toluene and stirred at 110 °C overnight. The reaction mixture was allowed to cool to room temperature and then concentrated under reduced pressure. The crude product was chromatographically purified on a silica gel column eluting with dichloromethane/petroleum ether (1/1, v/v) as the eluent to afford compound 4 as a red solid (1.4 g, 82.0% yield). ¹H NMR (400 MHz, CDCl₃) δ 7.74 (s, 2H), 7.37 (s, 4H), 2.68 (t, *J* = 7.7 Hz, 4H), 1.66 (m, 4H), 1.37 – 1.23 (m, 36H), 0.88 (m, 6H). ¹³C NMR (101 MHz, CDCl₃) δ 152.26, 152.13, 144.68, 143.03, 142.51, 141.33, 133.76, 132.55, 129.14, 127.09, 123.02, 122.72, 120.26, 32.01, 30.44, 30.33, 29.77, 29.74, 29.68, 29.52, 29.45, 29.31, 22.78, 14.22.

Synthesis of compound 4. Compound 3 (1.2 g, 1.1 mmol) and triphenylphosphine (5.8 g, 22 mmol) were dissolved in the *o*-dichlorobenzene (*o*-DCB, 20 mL) under nitrogen. After being heated at 200 °C for 12 h, the aqueous phase was extracted with dichloromethane and the organic layer was dried over Na₂SO₄ and filtered. After removing the solvent, the red residue was added into a two-necked round bottom flask. 5-(iodomethyl) undecane (2.9 g, 9.9 mmol), sodium hydroxide (440 mg, 11 mmol) and DMF (30 mL) were added and the mixture was deoxygenated with argon for 15 mins. The mixture was refluxed at 90 °C for 3 days. After removing the solvent from the filtrate, the residue was extracted with ethyl acetate and H₂O. The organic layers were combined and dried over MgSO₄, filtered and purified with column chromatography on silica gel using dichloromethane/petroleum ether (1/5, v/v) as the eluent to give a red solid 4 (575 mg, 32% yield). ¹H NMR (400 MHz, CDCl₃) δ 7.08 (s, 2H), 4.69 (d, *J* = 8

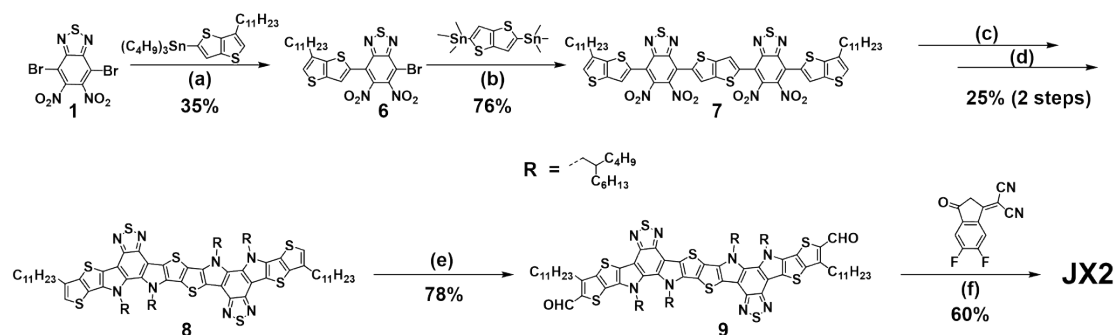
Hz, 4H), 4.52 (d, $J = 7.5$ Hz, 4H), 2.94 (t, $J = 7.7$ Hz, 4H), 2.24 – 2.14 (m, 2H), 1.85 (m, 8H), 1.30 (m, 40H), 1.15 – 0.84 (m, 54H), 0.76 – 0.50 (m, 34H). ^{13}C NMR (101 MHz, CDCl_3) δ 147.83, 147.48, 143.96, 137.70, 134.80, 132.34, 128.67, 125.38, 123.43, 122.57, 121.99, 111.39, 110.93, 54.92, 53.99, 39.43, 38.87, 31.98, 31.58, 30.12, 29.96, 29.86, 29.79, 29.77, 29.75, 29.72, 29.63, 29.56, 29.46, 29.42, 29.34, 22.83, 22.74, 22.65, 22.51, 14.17, 14.06, 14.03, 13.73, 13.69.

Synthesis of compound 5. Under the protection of argon, phosphorus oxychloride (0.2 mL) was added to a solution of compound 4 (200 mg, 0.12 mmol, 1.0 eq.) and *N, N*-Dimethylformamide (DMF, 0.3 mL) in 1, 2-dichloroethane ($\text{ClCH}_2\text{CH}_2\text{Cl}$, 10 mL). The resulting mixture was stirred and heated to reflux for 12 h, then was cooled to 0 °C. The resulting mixture was slowly added a saturated solution sodium acetate (40 mL), then was stirred at room temperature for 2 h. The resulting mixture was extracted with dichloromethane and the organic layer was dried over anhydrous Na_2SO_4 for 1 h. After removal of solvent, the crude product was then purified by column chromatography on silica gel with dichloromethane as eluent to afford compound 5 as a red solid (169 mg, 82%). ^1H NMR (400 MHz, CDCl_3) δ 10.16 (s, 2H), 4.70 (d, $J = 7.6$ Hz, 4H), 4.53 (d, $J = 7.4$ Hz, 4H), 3.69 – 3.04 (m, 4H), 2.22 – 2.12 (m, 2H), 2.05 – 1.73 (m, 8H), 1.31 – 1.25 (m, 40H), 1.05 – 0.78 (m, 54H), 0.75 – 0.53 (m, 34H). ^{13}C NMR (101 MHz, CDCl_3) δ 182.20, 147.65, 147.49, 143.84, 138.73, 138.65, 138.53, 137.62, 131.14, 130.93, 126.17, 122.80, 113.57, 110.39, 54.94, 54.34, 39.62, 38.95, 31.96, 31.72, 31.55, 30.07, 29.77, 29.73, 29.69, 29.67, 29.62, 29.45, 29.39, 27.15, 22.83, 22.73, 22.50, 14.15, 14.01, 13.71.

Synthesis of compound JX1. Under the protection of argon, dry pyridine (0.2 mL) was added to a solution of compound 5 (100 mg, 0.059 mmol, 1.0 eq.) and 2-(3-oxo-2,3-

dihydro-1*H*-cyclopenta [*b*] naphthalen-1-ylidene) malononitrile (69 mg, 0.30 mmol 5.0 eq.) in chloroform (CHCl₃, 10 mL). The resulting mixture was stirred and heated to reflux for 12 h. After being cooled to room temperature, the solvent was removed under vacuum. The crude product was then purified by column chromatography on silica gel with hexanes/dichloromethane (*v/v* = 1:2) as eluent to afford **JX1** as a black and green solid (75 mg, 60%). ¹H NMR (400 MHz, CDCl₃) δ 9.20 (s, 2H), 8.56 (t, *J* = 8.3 Hz, 2H), 7.72 (d, *J* = 8.1 Hz, 2H), 4.64 (m, 8H), 3.36 (m, 4H), 2.18 (m, 2H), 1.85 (m, 6H), 1.56 (m, 7H), 1.28 (m, 53H), 0.87 (m, 36H), 0.66 (m, 34H). ¹³C NMR (101 MHz, CDCl₃) δ 185.69, 159.56, 155.49, 155.41, 153.02, 152.98, 152.88, 152.84, 147.63, 147.48, 144.95, 143.77, 141.30, 139.92, 139.75, 136.56, 136.48, 135.55, 135.17, 134.57, 134.54, 130.57, 126.93, 123.89, 119.59, 115.57, 115.52, 114.97, 114.90, 114.68, 112.53, 112.34, 110.70, 77.33, 77.22, 77.02, 76.70, 67.30, 55.08, 54.47, 39.48, 39.04, 32.25, 31.92, 31.51, 30.17, 29.78, 29.71, 29.67, 29.65, 29.40, 29.36, 28.07, 22.77, 22.69, 22.47, 14.11, 13.98, 13.69.

2.2 Synthesis of JX2



Scheme S2. The overall synthetic route to JX2. Reagents and conditions: a) $\text{Pd}_2(\text{dba})_3$, $\text{P}(o\text{-tolyl})_3$, toluene, 60 °C, 2 days; b) $\text{Pd}_2(\text{dba})_3$, $\text{P}(o\text{-tolyl})_3$, toluene, reflux, overnight; c) PPh_3 , *o*-DCB, reflux, 12 h; d) NaOH, DMF, 5-(Iodomethyl)undecane, 90 °C, 3 days; e) POCl_3 , DMF, $\text{ClCH}_2\text{CH}_2\text{Cl}$, reflux, 12 h; f) 2-(6,7-difluoro-3-oxo-2,3-dihydro-1H-cyclopenta[*b*] naphthalen-1-ylidene) malononitrile, pyridine, CHCl_3 , reflux, 12 h.

Synthesis of compound 6. Under the protection of argon, compound 1 (6.3 g, 16.41 mmol), tributyl(6-undecylthieno[3,2-*b*]thiophen-2-yl)stannane (6.7 g, 11.48 mmol), $\text{Pd}_2(\text{dba})_3$ (601 mg, 0.656 mmol), $\text{P}(o\text{-tolyl})_3$ (799 mg, 2.63 mmol) were dissolved in 80 mL of dry toluene and stirred at 60 °C for 2 days. The reaction mixture was allowed to cool to room temperature and then concentrated under reduced pressure. The crude product was chromatographically purified on a silica gel column eluting with dichloromethane/petroleum ether (1/5, *v/v*) as the eluent to afford compound 6 as a red solid (2.4 g, 35.0% yield). ^1H NMR (400 MHz, CDCl_3) δ 7.67(s, 1H), 7.15(s, 1H), 2.74(t, $J = 8$ Hz, 2H), 1.80 – 1.73 (m, 2H) 1.43 – 1.27 (m, 19H). ^{13}C NMR (101 MHz, CDCl_3) δ 152.30, 151.05, 144.92, 144.45, 141.29, 139.11, 135.12, 129.50, 125.54, 124.47, 122.58, 108.48, 31.99, 29.82, 29.74, 29.71, 29.66, 29.45, 29.43, 29.37, 28.59, 22.78, 14.24.

Synthesis of compound 7. Under the protection of argon, compound 6 (1.2 g, 2 mmol), compound 4 (423 mg, 0.91 mmol), Pd₂(dba)₃ (33 mg, 0.0364 mmol), P(*o*-tolyl)₃ (44 mg, 0.15 mmol) were dissolved in 20 mL of dry toluene and stirred at 110 °C overnight. The reaction mixture was allowed to cool to room temperature and then concentrated under reduced pressure. The crude product was chromatographically purified on a silica gel column eluting with dichloromethane/petroleum ether (1/1, v/v) as the eluent to afford compound 7 as a red solid (811 mg, 76.0% yield). ¹H NMR (400 MHz, CDCl₃) δ 7.76 (s, 2H), 7.75 (s, 2H), 7.20 (s, 2H), 2.78 (t, *J* = 7.7 Hz, 4H), 1.79 (m, 4H), 1.42 – 1.27 (m, 32H), 0.88 (t, *J* = 6.3 Hz, 6H). ¹³C NMR (101 MHz, CDCl₃) δ 151.11, 143.56, 142.05, 141.11, 140.38, 138.18, 134.12, 132.73, 129.92, 128.89, 124.50, 123.37, 121.97, 121.47, 119.33, 30.89, 28.80, 28.64, 28.61, 28.56, 28.36, 28.33, 27.54, 21.67, 13.10.

Synthesis of compound 8. Compound 7 (1.05 g, 0.89 mmol) and triphenylphosphine (4.7 g, 17.9 mmol) were dissolved in the *o*-dichlorobenzene (*o*-DCB, 15 mL) under nitrogen. After being heated at 200 °C for 12 h, the aqueous phase was extracted with dichloromethane and the organic layer was dried over Na₂SO₄ and filtered. After removing the solvent, the red residue was added into a two-necked round bottom flask. 5-(iodomethyl) undecane (2.37 g, 8 mmol), sodium hydroxide (356 mg, 8.9 mmol) and DMF (30 mL) were added and the mixture was deoxygenated with argon for 15 mins. The mixture was refluxed at 90 °C for 3 days. After removing the solvent from the filtrate, the residue was extracted with ethyl acetate and H₂O. The organic layers were combined and dried over MgSO₄, filtered and purified with column chromatography on silica gel using dichloromethane/petroleum ether (1/5, v/v) as the eluent to give a red solid 8 (382 mg, 25% yield). ¹H NMR (400 MHz, CDCl₃) δ 7.04 (s, 2H), 4.70 (d, *J* = 5.8 Hz, 4H), 4.65 (d, *J* = 4.9 Hz, 4H), 2.84 (t, *J* = 5.8 Hz, 4H), 2.17 (m, 4H), 1.87 (m,

4H), 1.35 – 1.28 (m, 27H), 0.98 – 0.81 (m, 71H), 0.70 – 0.58 (m, 28H). MS (*m/z*, MALDI): Calc. for C₁₀₀H₁₄₈N₈S₈: 1718.82. Found: 1717.9588.

Synthesis of compound 9. Under the protection of argon, phosphorus oxychloride (0.2 mL) was added to a solution of compound 8 (200 mg, 0.116 mmol, 1.0 eq.) and *N, N*-Dimethylformamide (DMF, 0.3 mL) in 1, 2-dichloroethane (ClCH₂CH₂Cl, 10 mL). The resulting mixture was stirred and heated to reflux for 12 h, then was cooled to 0 °C. The resulting mixture was slowly added a saturated solution sodium acetate (40 mL), then was stirred at room temperature for 2 h. The resulting mixture was extracted with dichloromethane and the organic layer was dried over anhydrous Na₂SO₄ for 1 h. After removal of solvent, the crude product was then purified by column chromatography on silica gel with hexanes/dichloromethane (*v/v* = 2:1) as eluent to afford compound 9 as a red solid (161 mg, 78%). ¹H NMR (400 MHz, CDCl₃) δ 10.15 (s, 2H), 4.69 (dd, *J* = 17.5, 7.8 Hz, 8H), 3.21 (t, *J* = 7.7 Hz, 4H), 2.14 (m, 4H), 1.94 (m, 4H), 1.28 (d, *J* = 9.7 Hz, 27H), 1.15 – 0.82 (m, 71H), 0.64 (m, 28H). MS (*m/z*, MALDI): Calc. for C₁₀₂H₁₄₈N₈O₂S₈: 1774.84. Found: 1773.9478.

Synthesis of compound JX2. Under the protection of argon, dry pyridine (0.2 mL) was added to a solution of compound 9 (100 mg, 0.0563 mmol, 1.0 eq.) and 2-(3-oxo-2,3-dihydro-1*H*-cyclopenta [*b*] naphthalen-1-ylidene) malononitrile (65 mg, 0.282 mmol 5.0 eq.) in chloroform (CHCl₃, 10 mL). The resulting mixture was stirred and heated to reflux for 12 h. After being cooled to room temperature, the solvent was removed under vacuum. The crude product was then purified by column chromatography on silica gel with hexanes/dichloromethane (*v/v* = 1:2) as eluent to afford JX2 as a black and purple solid (74 mg, 60%). ¹H NMR (400 MHz, CDCl₃) δ 9.14 (s, 2H), 8.55 (dd, *J* = 9.9, 6.5 Hz, 2H), 7.69 (t, *J* = 7.5 Hz, 2H), 4.76 (t, *J* = 8.1 Hz, 8H), 3.23 (t, *J* = 7.8 Hz, 4H), 2.32

– 2.08 (m, 4H), 1.88 (m, 4H), 1.53 (m, 5H), 1.35 – 1.23 (m, 28H), 1.21 – 0.78 (m, 68H),
0.67 (m, 25H). MS (*m/z*, MALDI): Calc. for C₁₂₆H₁₅₂F₄N₁₂O₂S₈: 2199.15761, found:
2198.9863.

3. Figures (S1-S31).

3.1 Photophysical properties of JX1 and JX2.

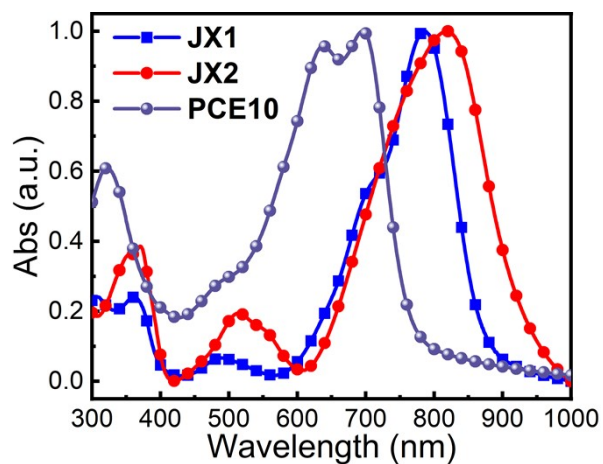


Figure S1. Normalized electron absorption spectra of PCE10, JX1 and JX2 thin films.

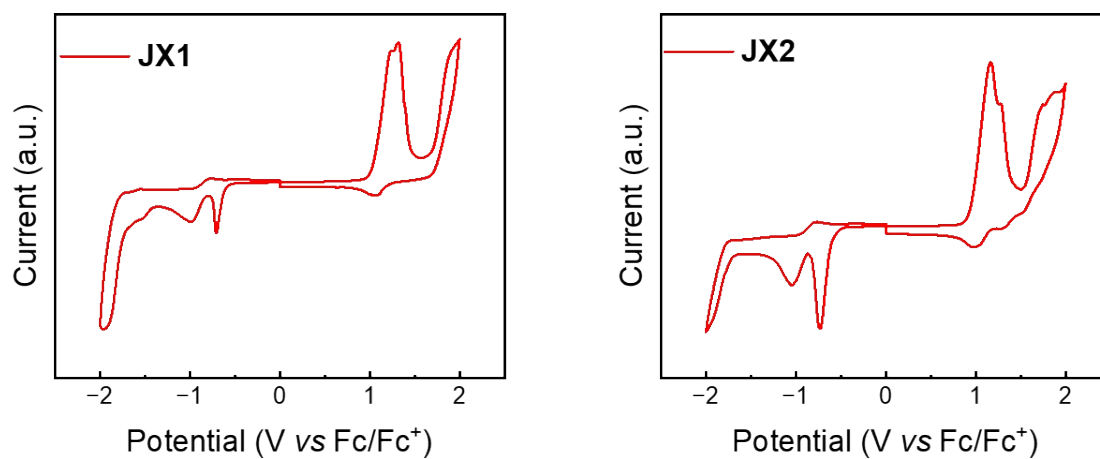


Figure S2. Cyclic voltammetry plots of JX1 and JX2 films.

3.2. Photovoltaic device performance.

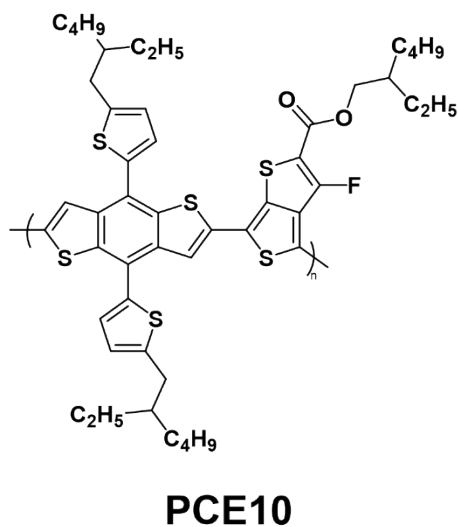


Figure S3. Structure of compound PCE10.

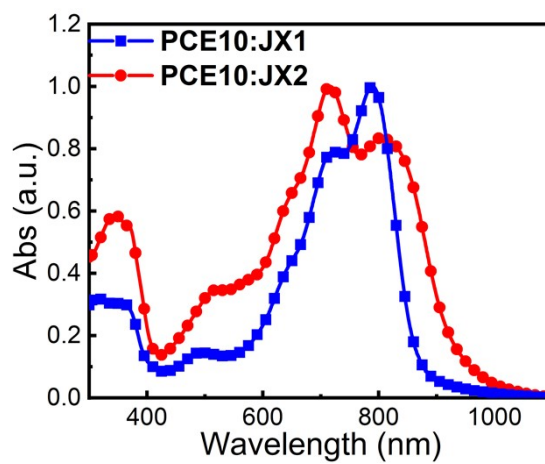


Figure S4. Normalized absorption spectra for blend films based on PCE10:JX1 and PCE10:JX2.

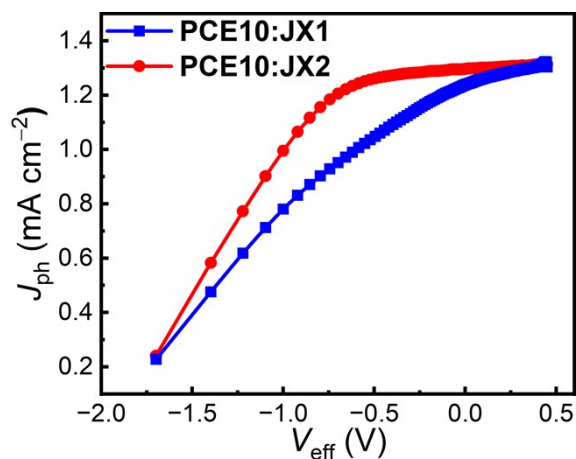


Figure S5. J_{ph} vs. V_{eff} curves of the optimized devices.

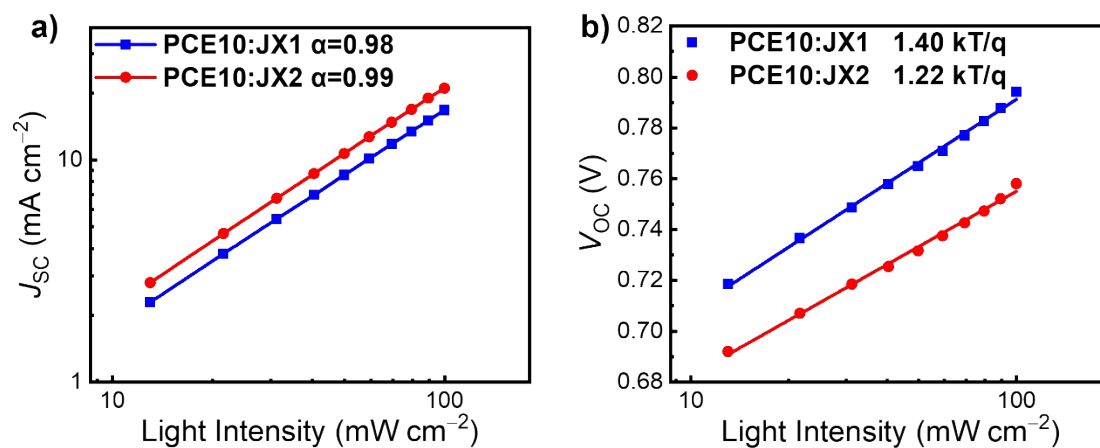


Figure S6. a) J_{SC} versus light intensity based on PCE10:JX1 and PCE10:JX2 at optimal conditions. α was obtained from pots of dependence of current density (J_{SC}) on P_{light} of optimized OSCs. If α gets close to 1, a negligible bimolecular recombination can be achieved. The α values from the PCE10:JX1 and PCE10:JX2 devices were determined to be 0.98 and 0.99, respectively. b) V_{OC} versus light intensity based on PCE10:JX1 and

PCE10:JX2 at optimal conditions. A slope close to kT/q indicates devices are dominated by bimolecular recombination and close to $2 kT/q$ suggests trap-assisted recombination is the dominating mechanism (where k is the Boltzmann's constant, T is the absolute temperature, and q is the elementary charge). The slope values from the PCE10:JX1 and PCE10:JX2 devices were determined to be 1.40, $1.22kT/q$, respectively.

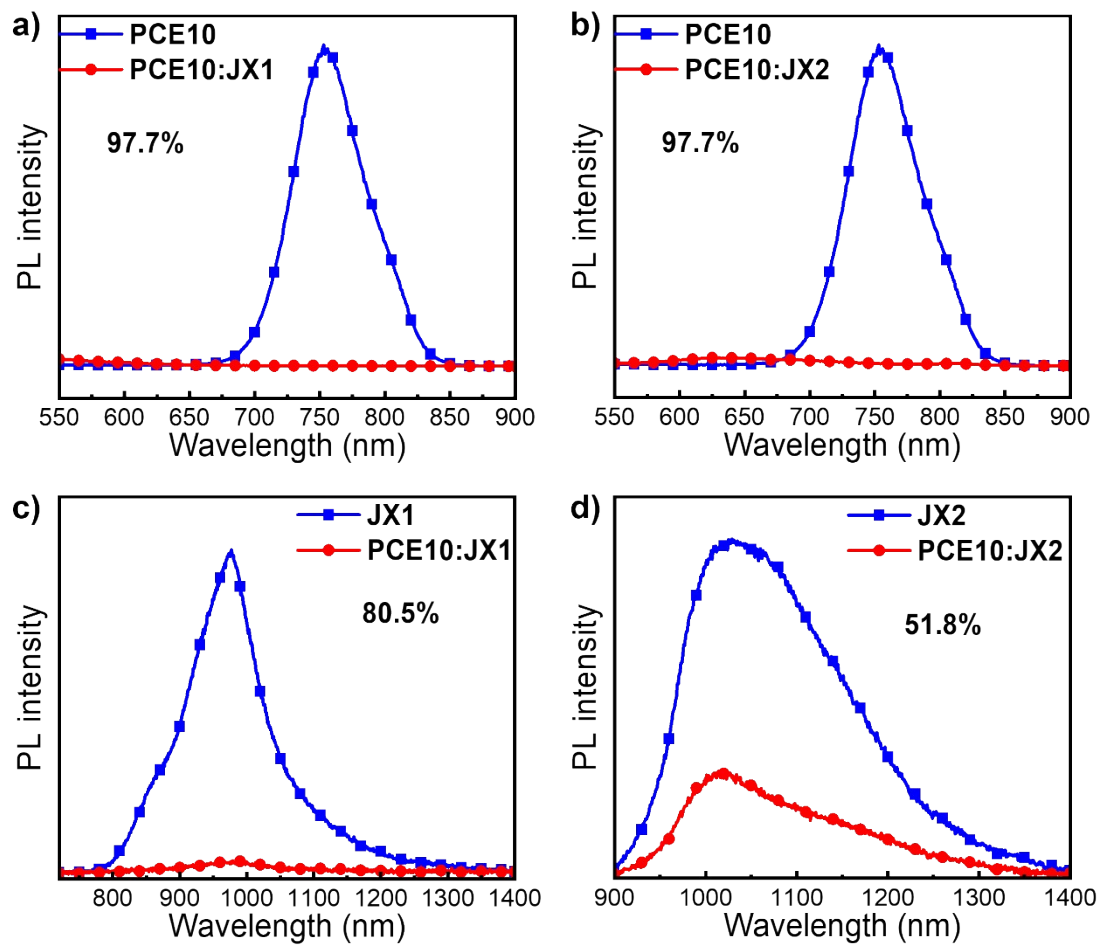


Figure S7. The photoluminescence (PL) spectra a) neat film of PCE10 and blend films of PCE10:JX1, b) neat film of PCE10 and blend films of PCE10:JX2, c) neat film of JX1 and blend films of PCE10:JX1, d) neat film of JX2 and blend films of PCE10:JX2. All these films were annealed upon 90 °C in glove box for 5 mins.

3.3. Morphology analysis.

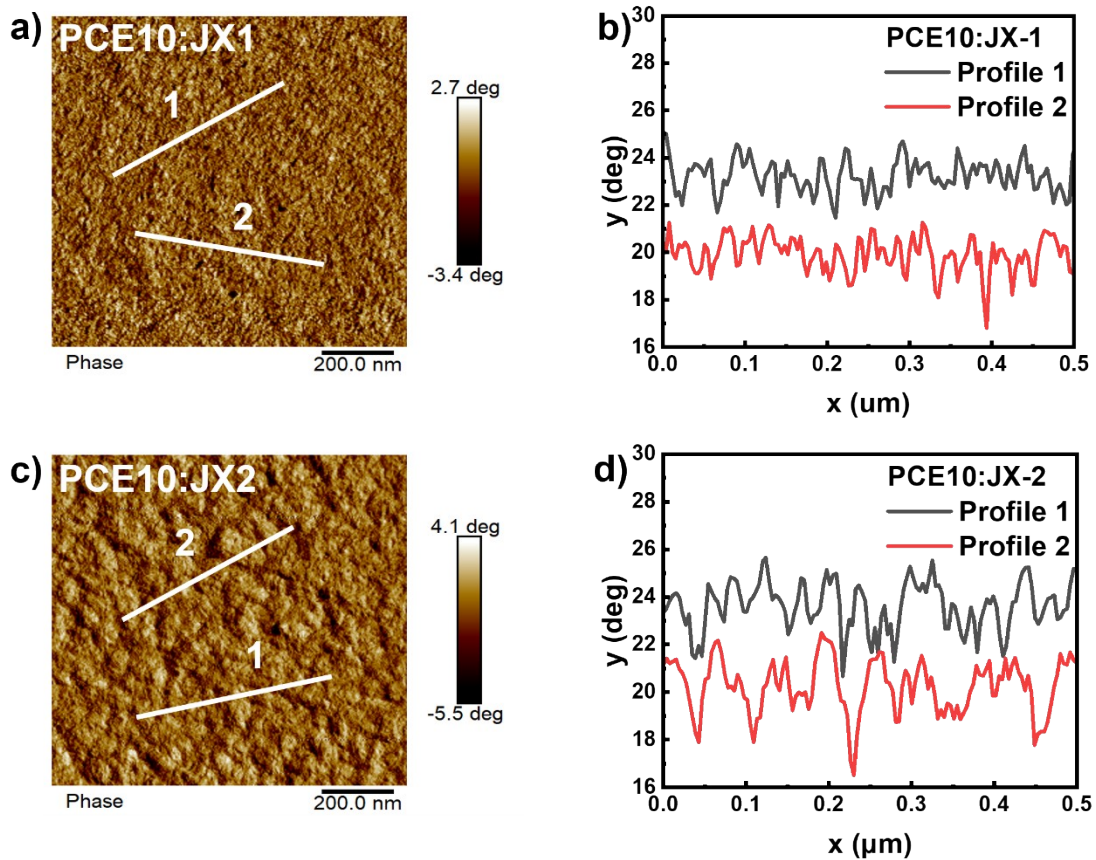


Figure S8. a) and c) AFM phase images. b) and d) The line profile to obtain the fibril width from the AFM phase images of PCE10:JX1 and PCE10:JX2 blended films.

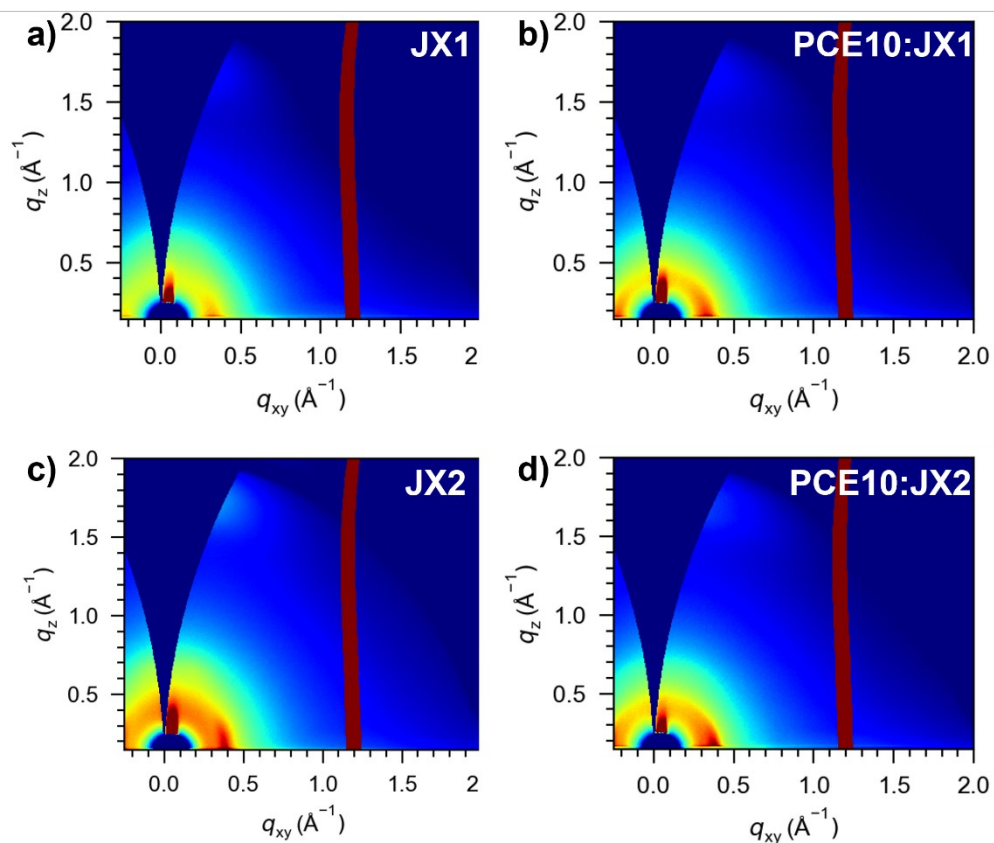


Figure S9. a) and c) GIWAXS images of neat JX1 and JX2. b) and d) GIWAXS images of optimized PCE10:JX1 and PCE10:JX2 blend films.

3.3. E_{loss} analysis.

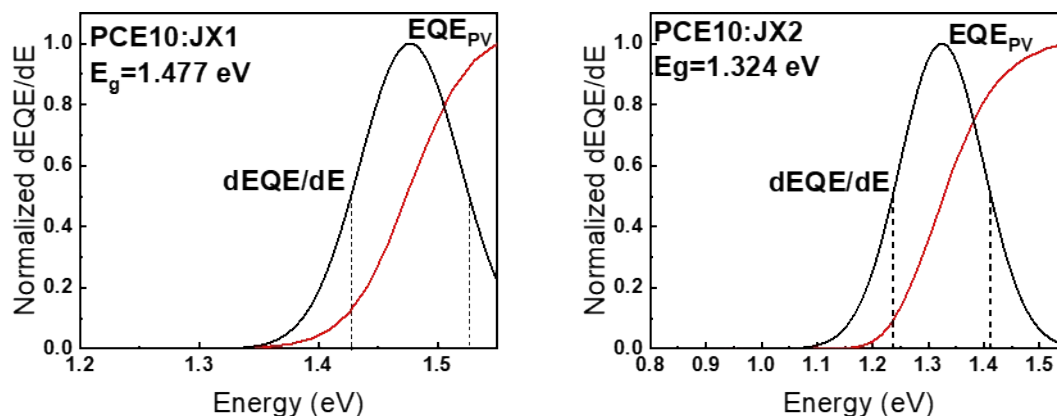


Figure S10. Details of optical E_g determination. E_g is estimated by by the derivatives of the EQE spectra of the blended films. The region between dashed lines are the part where the gap distribution probability is greater than half of the maximum, which is used for the optical gap calculation.

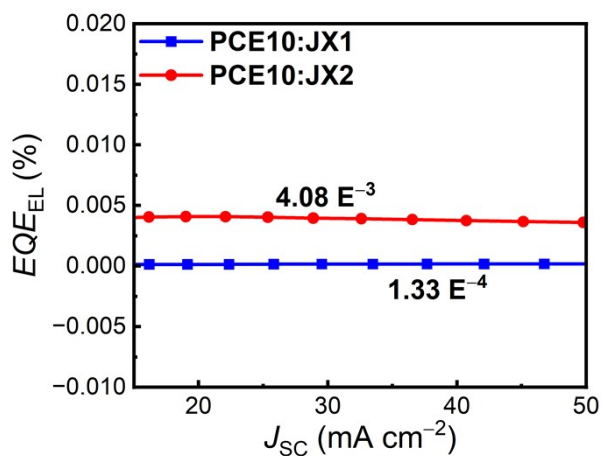


Figure S11. EQE_{EL} curves of OSCs at various current densities.

3.4. NMR and HR-MS spectra.

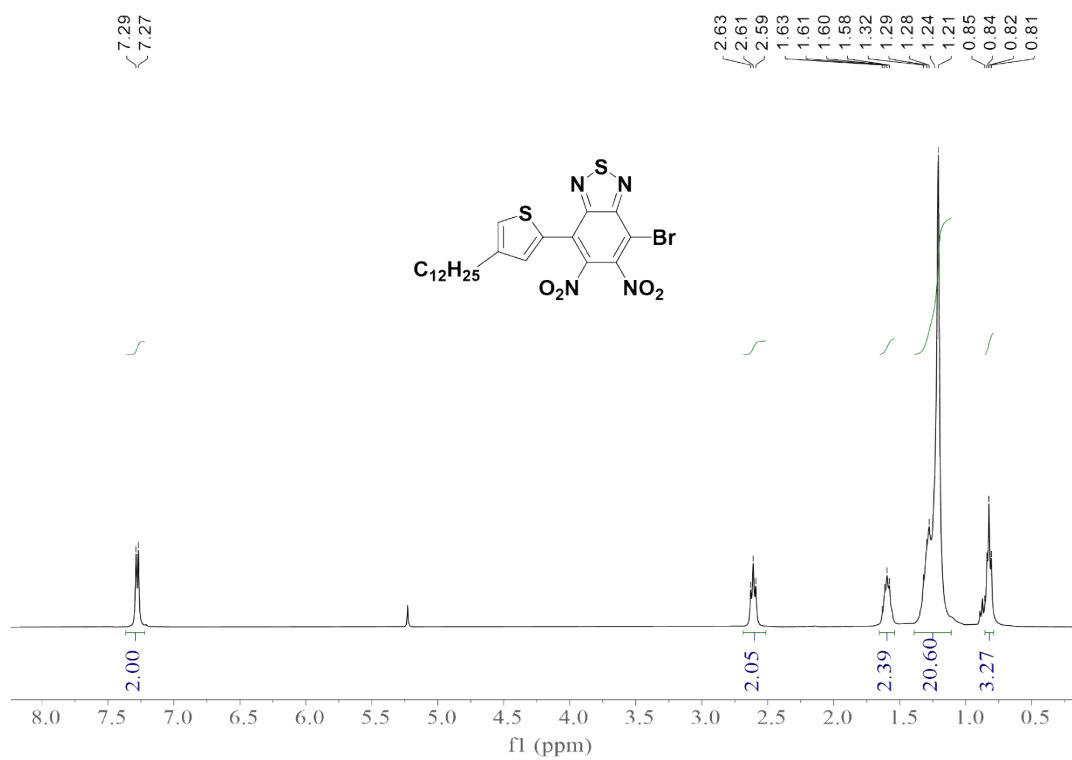


Figure S12. ¹H NMR spectrum of compound 2 at 300 K in CDCl₃.

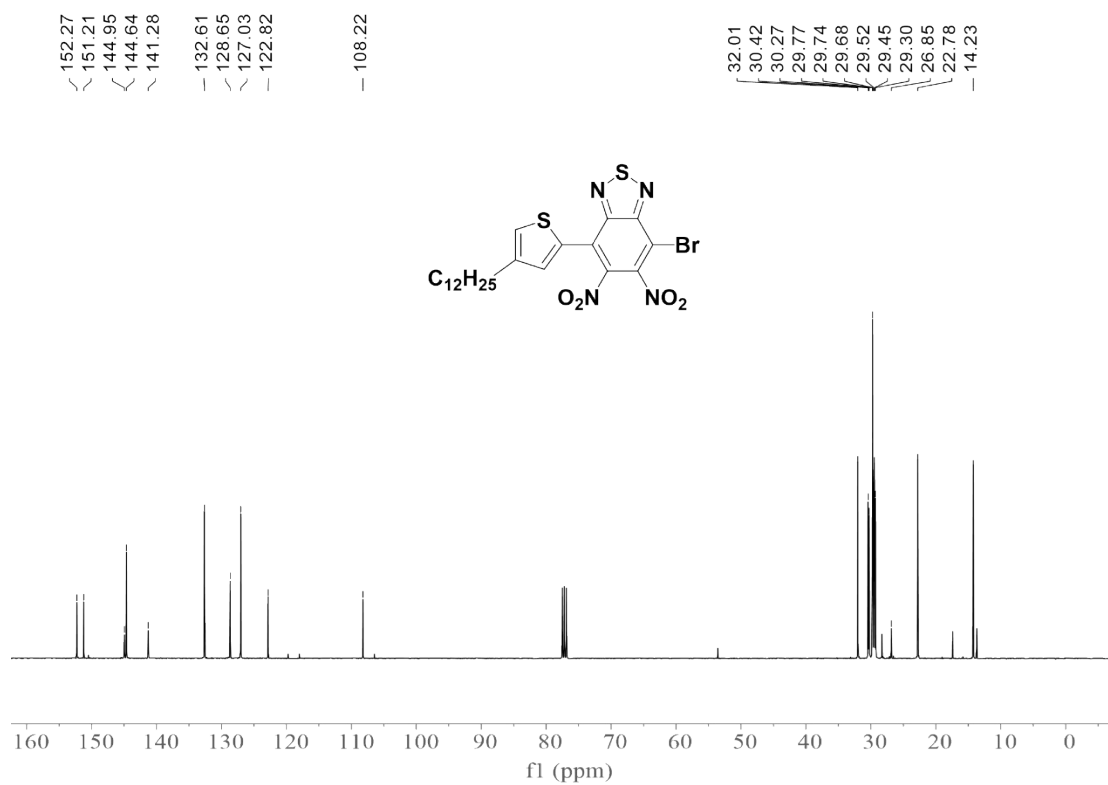


Figure S13. ^{13}C NMR spectrum of compound 2 at 300 K in CDCl_3 .

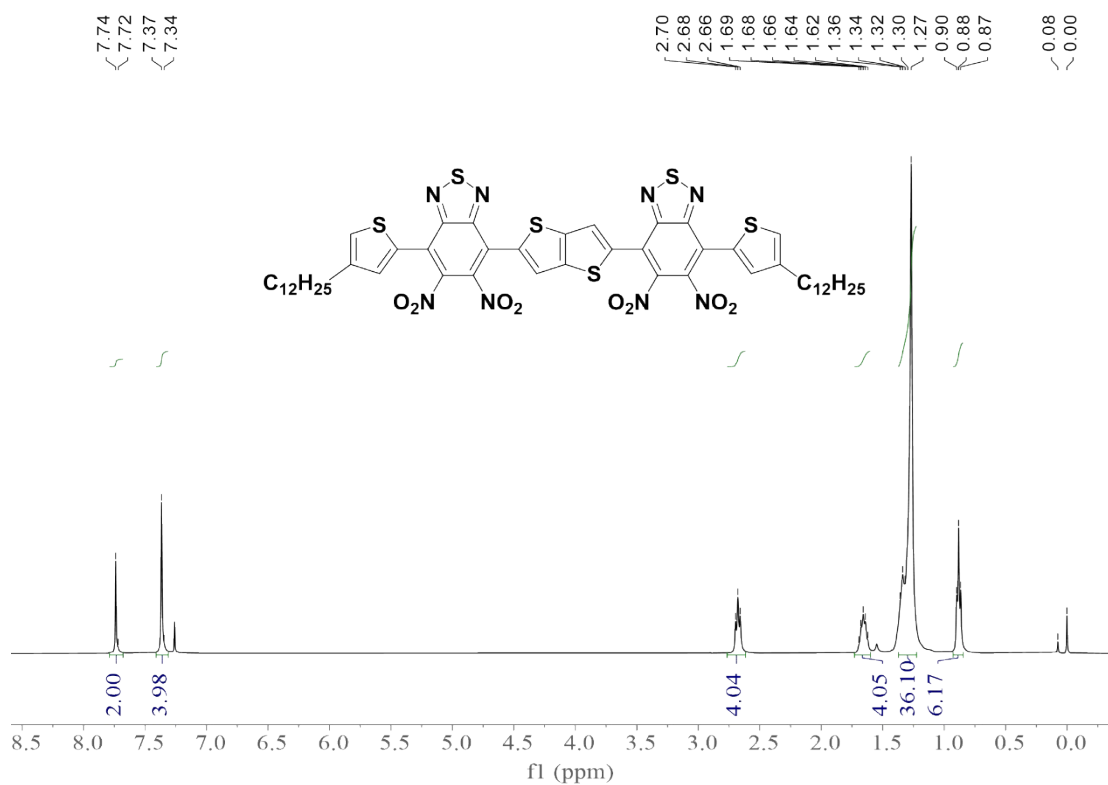


Figure S14. ^1H NMR spectrum of compound 3 at 300 K in CDCl_3 .

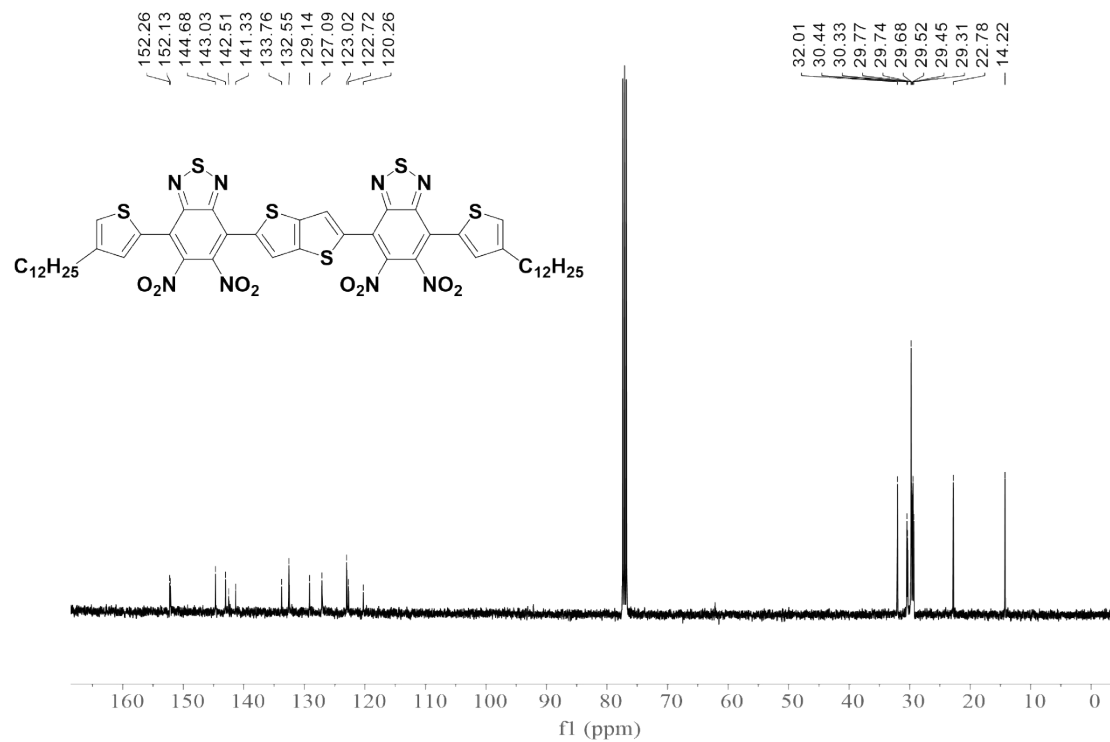


Figure S15. ¹³C NMR spectrum of compound 3 at 300 K in CDCl₃.

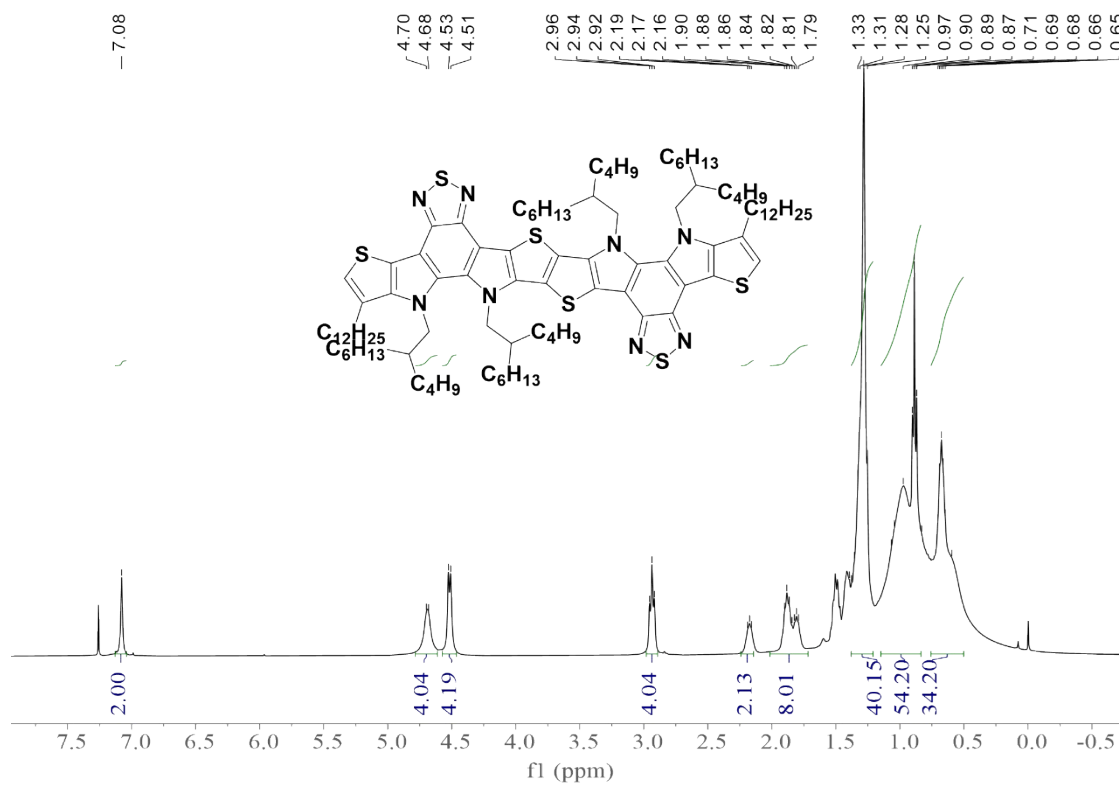


Figure S16. ¹H NMR spectrum of compound 4 at 300 K in CDCl₃.

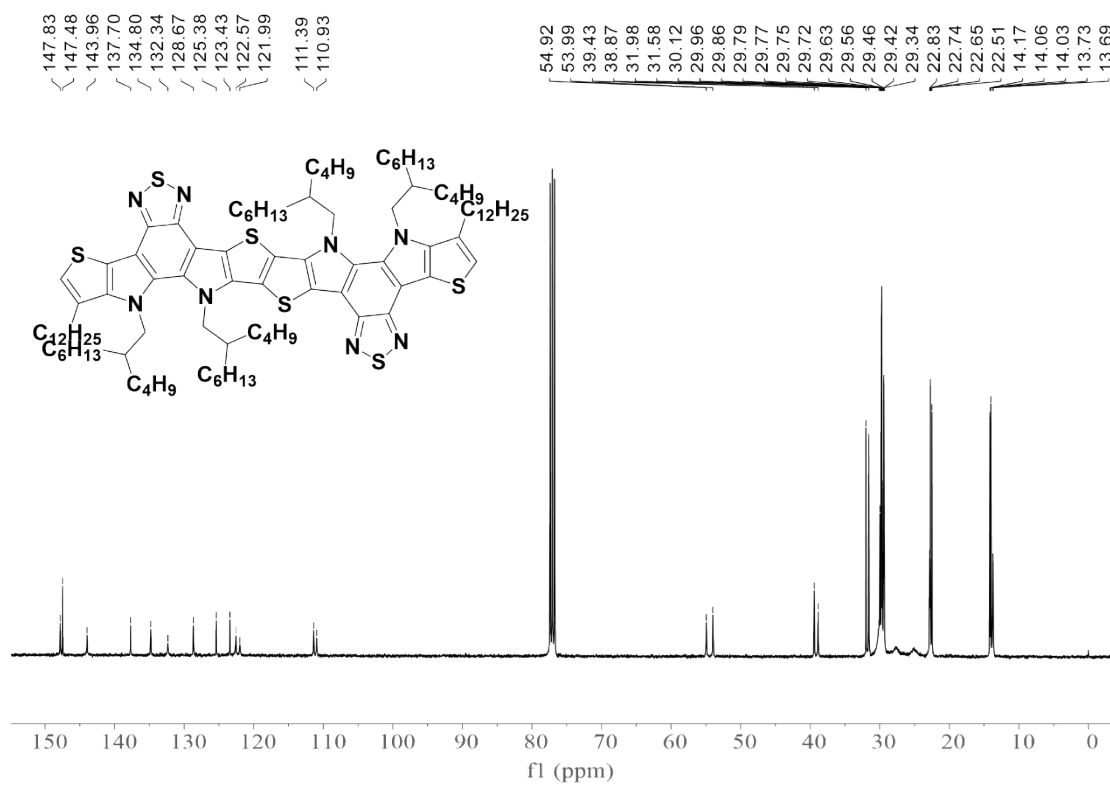


Figure S17. ^{13}C NMR spectrum compound 4 at 300 K in $CDCl_3$.

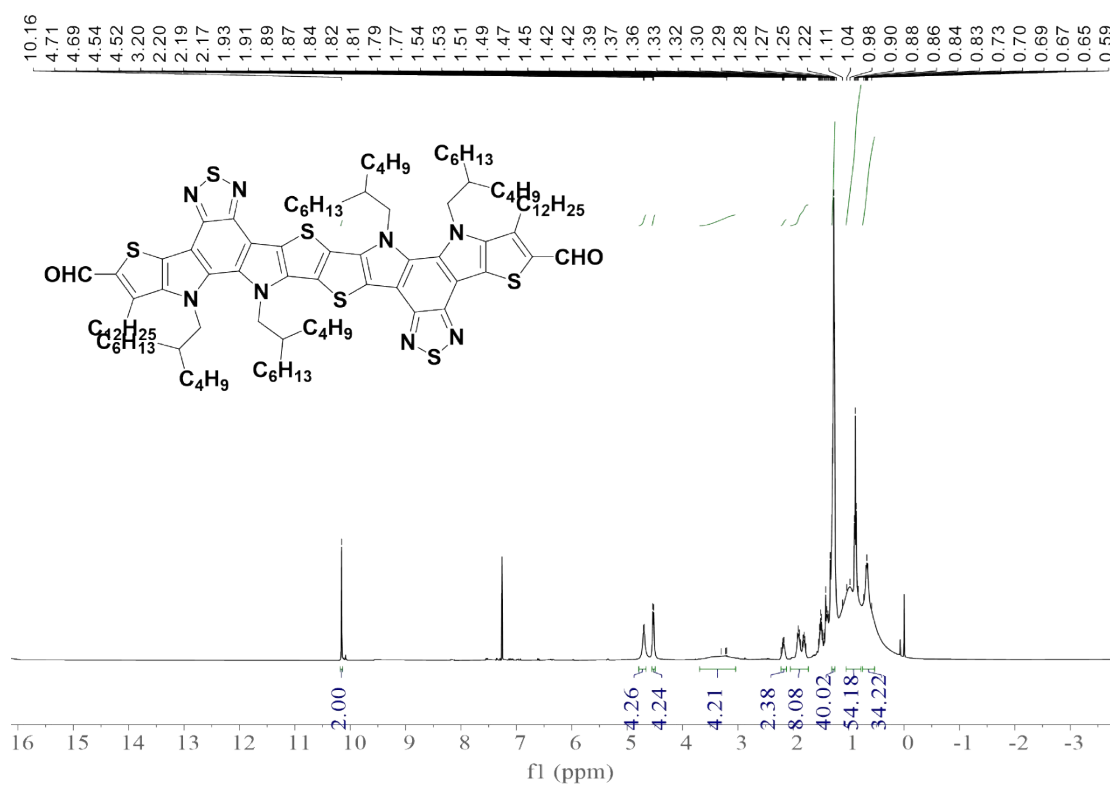


Figure S18. 1H NMR spectrum of compound 5 at 300 K in $CDCl_3$.

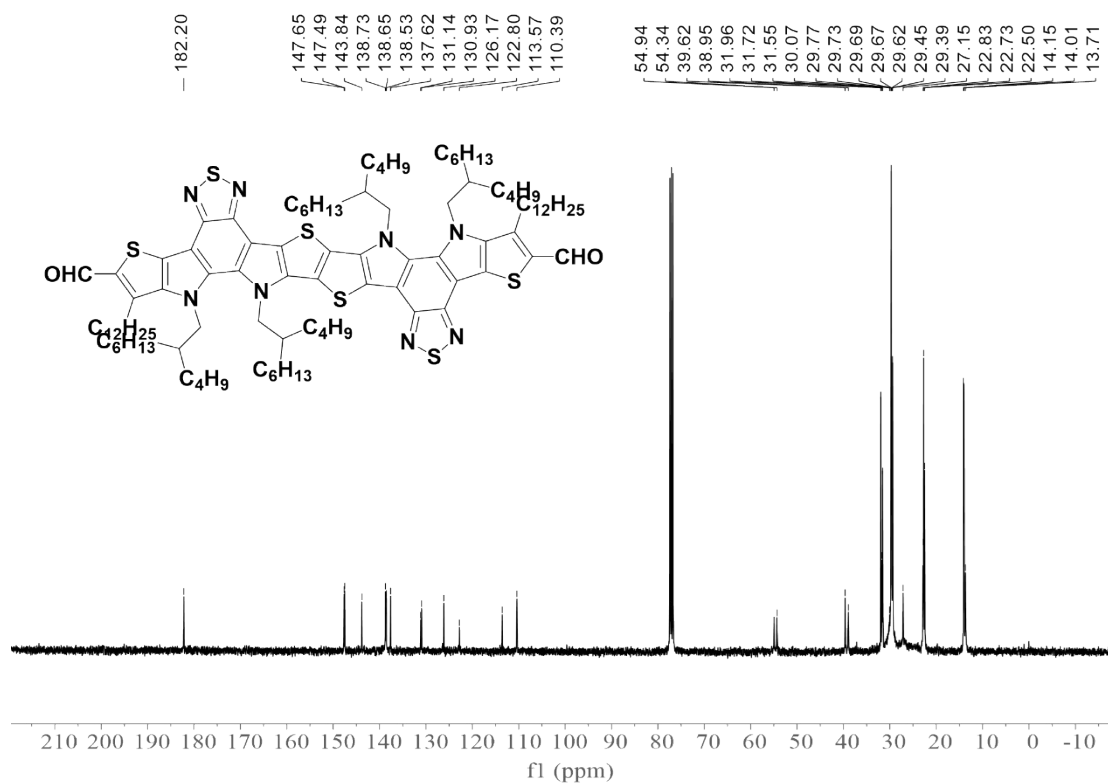


Figure S19. ¹³C NMR spectrum compound 5 at 300 K in CDCl₃.

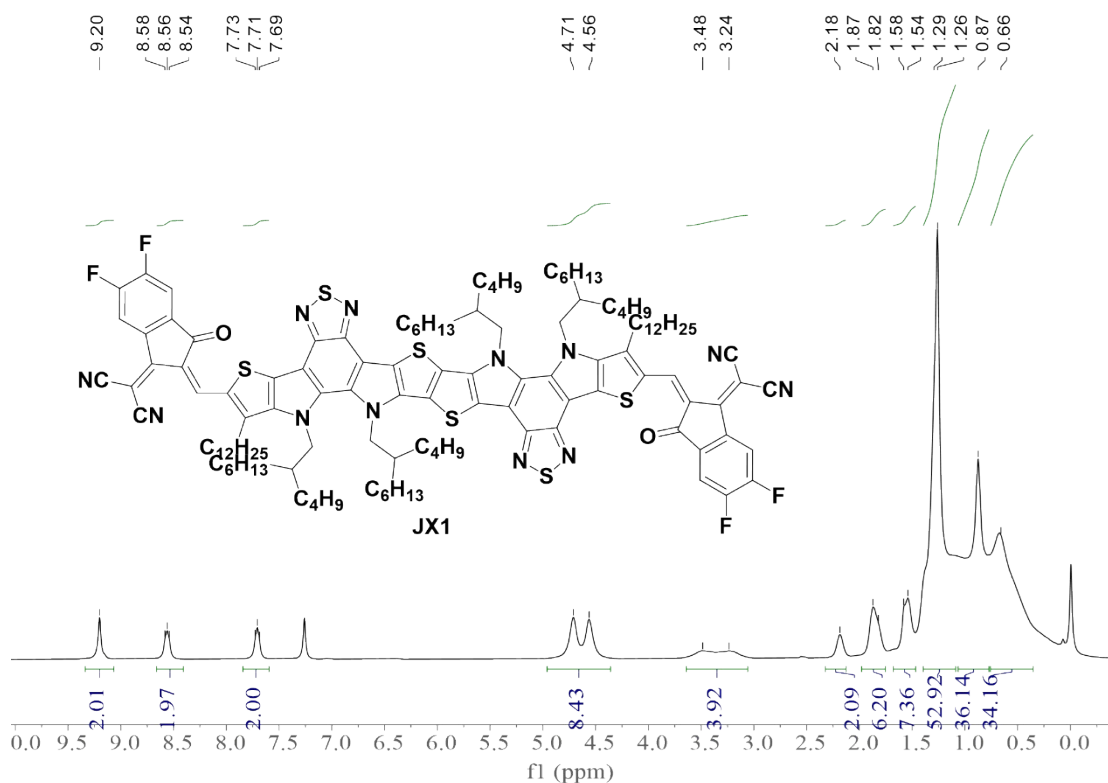


Figure S20. ¹H NMR spectrum of JX1 at 300 K in CDCl₃.

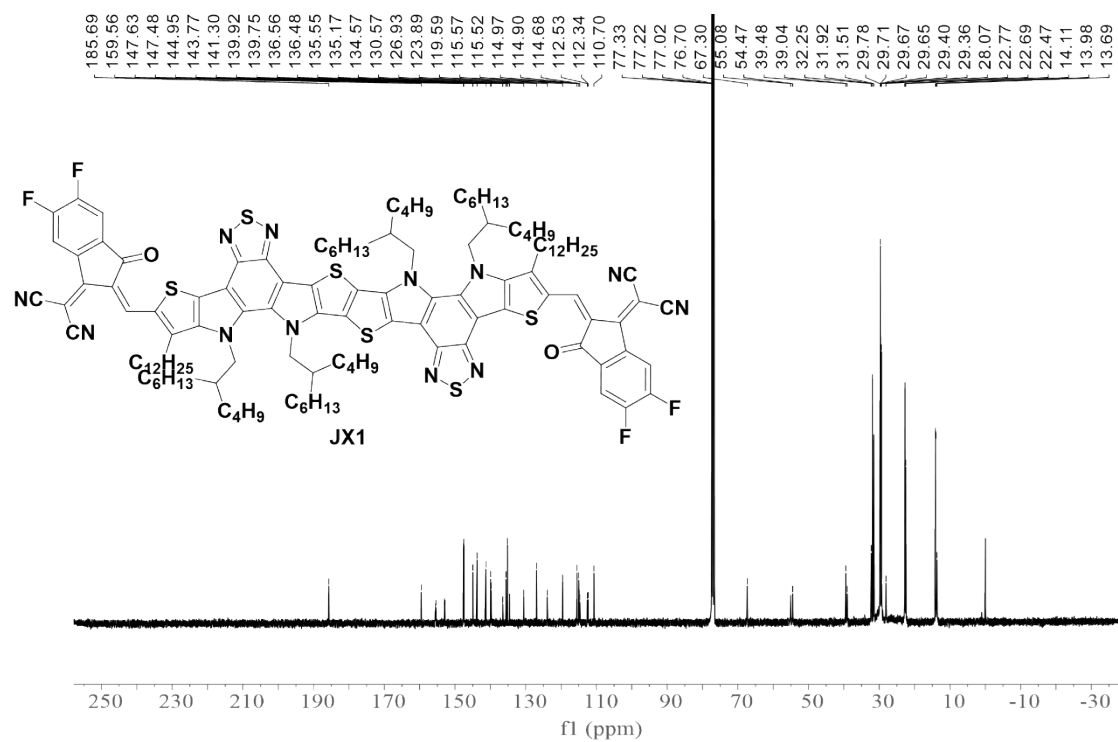


Figure S21. ^{13}C NMR spectrum JX1 at 300 K in $CDCl_3$.

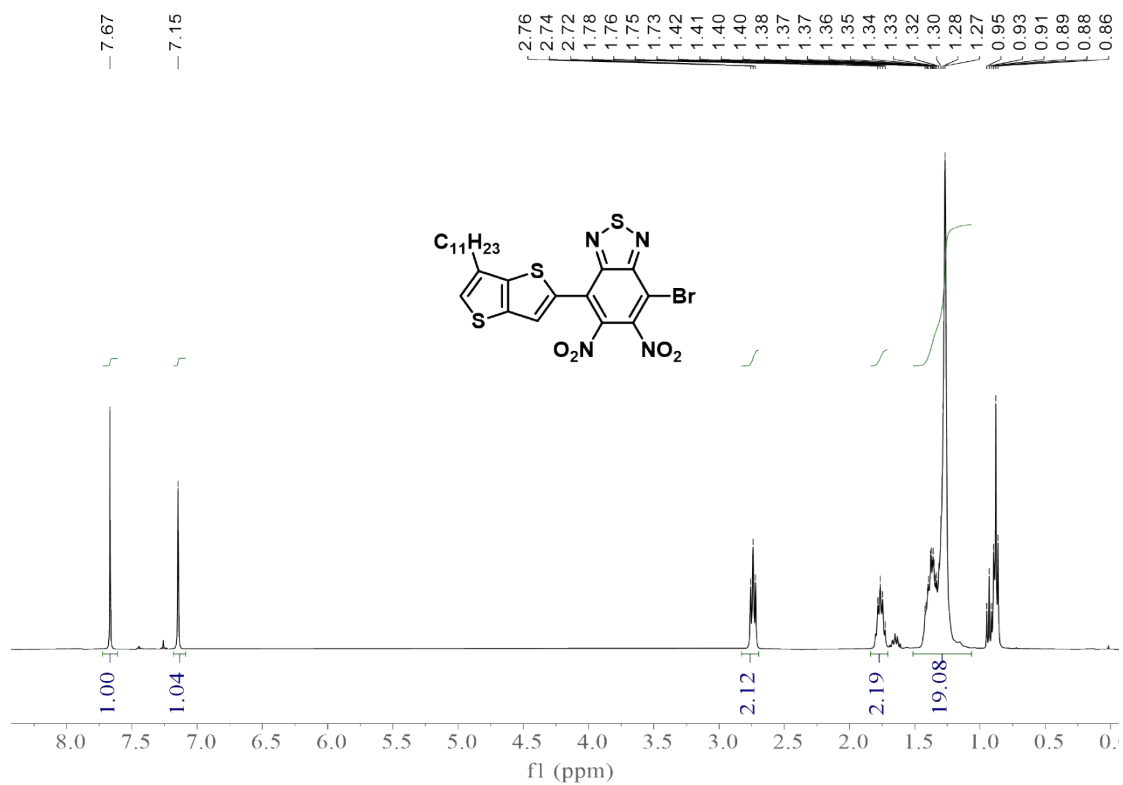


Figure S22. 1H NMR spectrum of compound 6 at 300 K in $CDCl_3$.

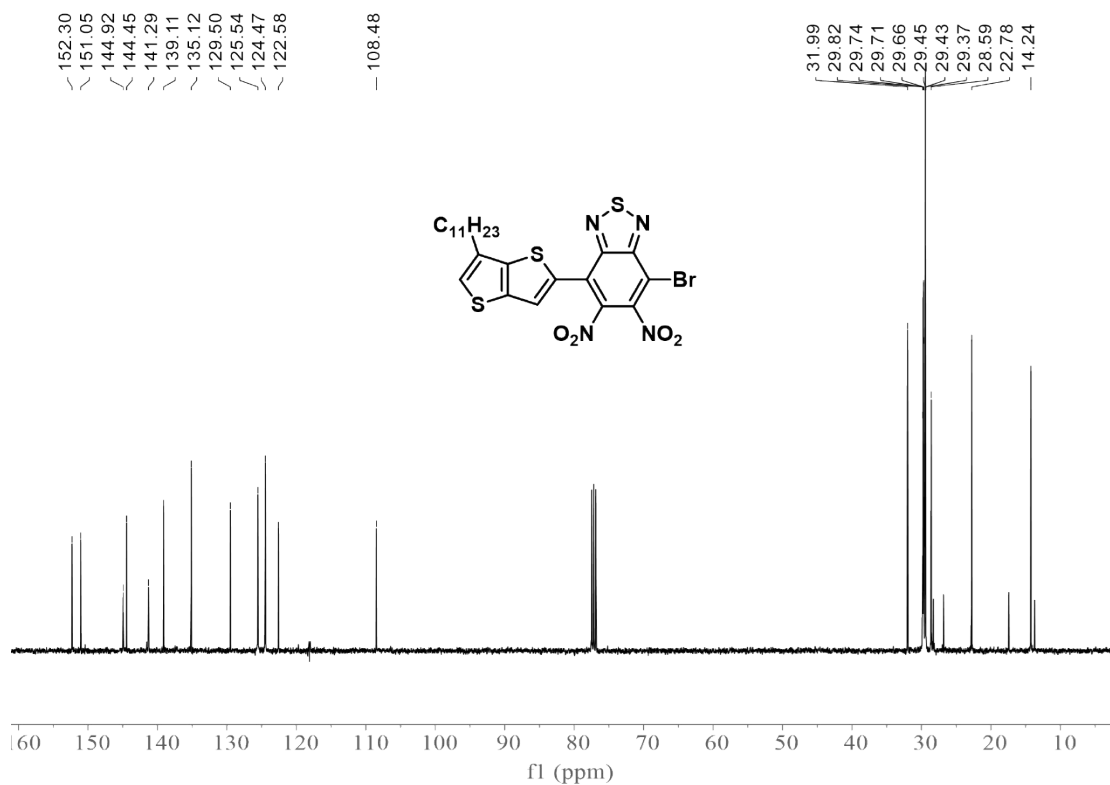


Figure S23. ^{13}C NMR spectrum compound 6 at 300 K in CDCl_3 .

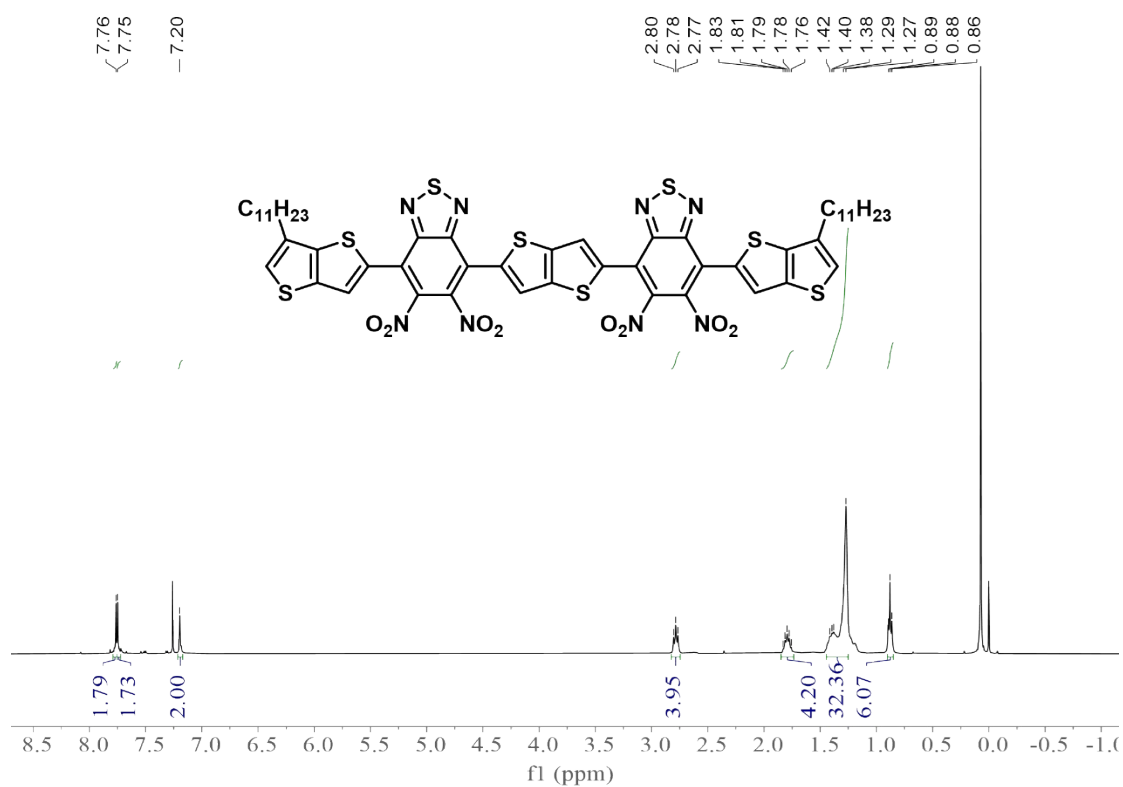


Figure S24. ^1H NMR spectrum of compound 7 at 300 K in CDCl_3 .

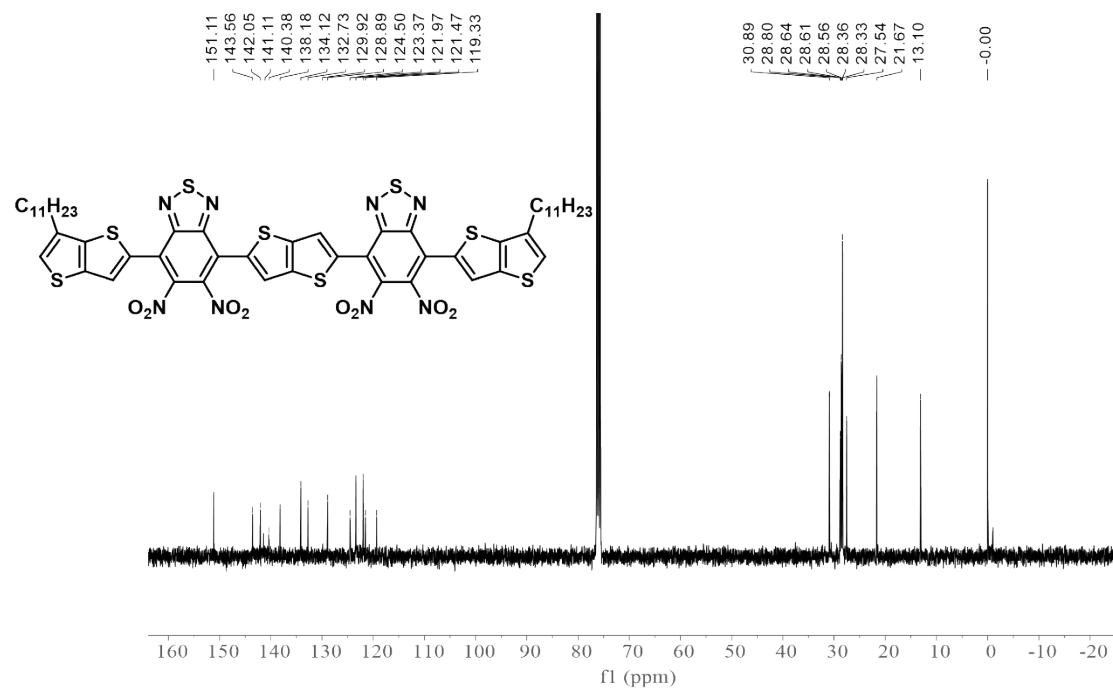


Figure S25. ¹³C NMR spectrum compound 7 at 300 K in CDCl₃.

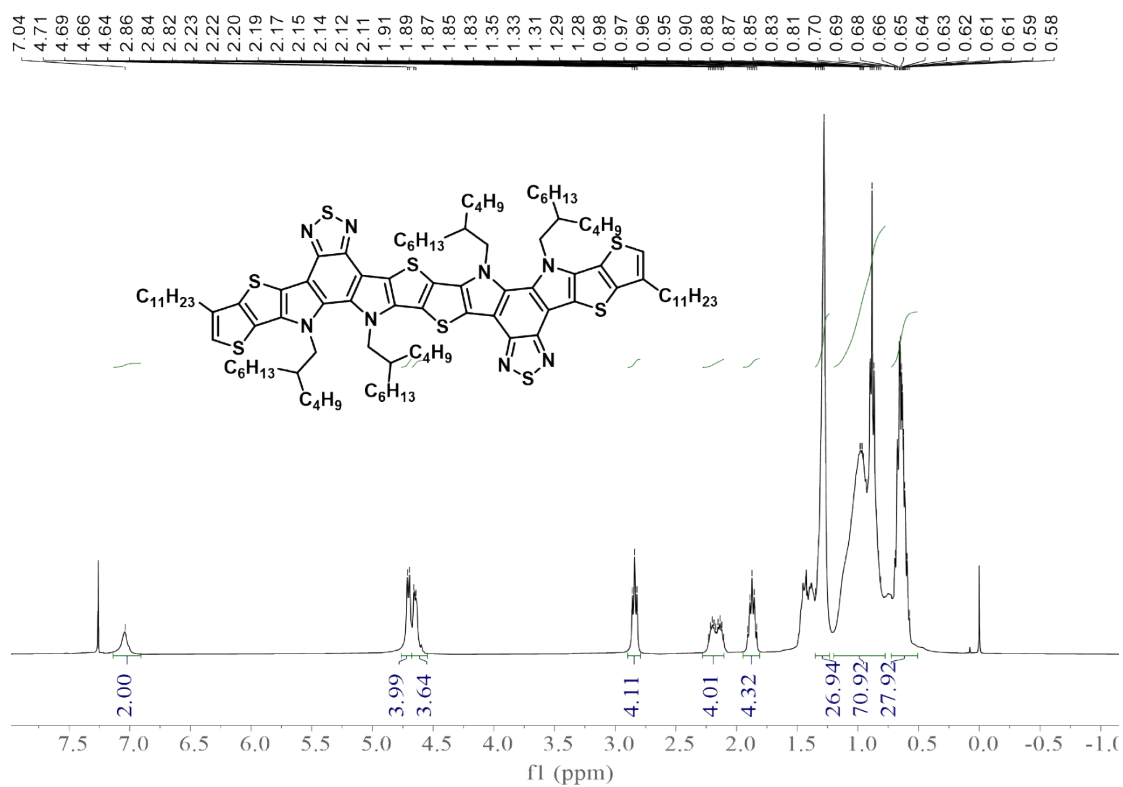


Figure S26. ¹H NMR spectrum of compound 8 at 300 K in CDCl₃.

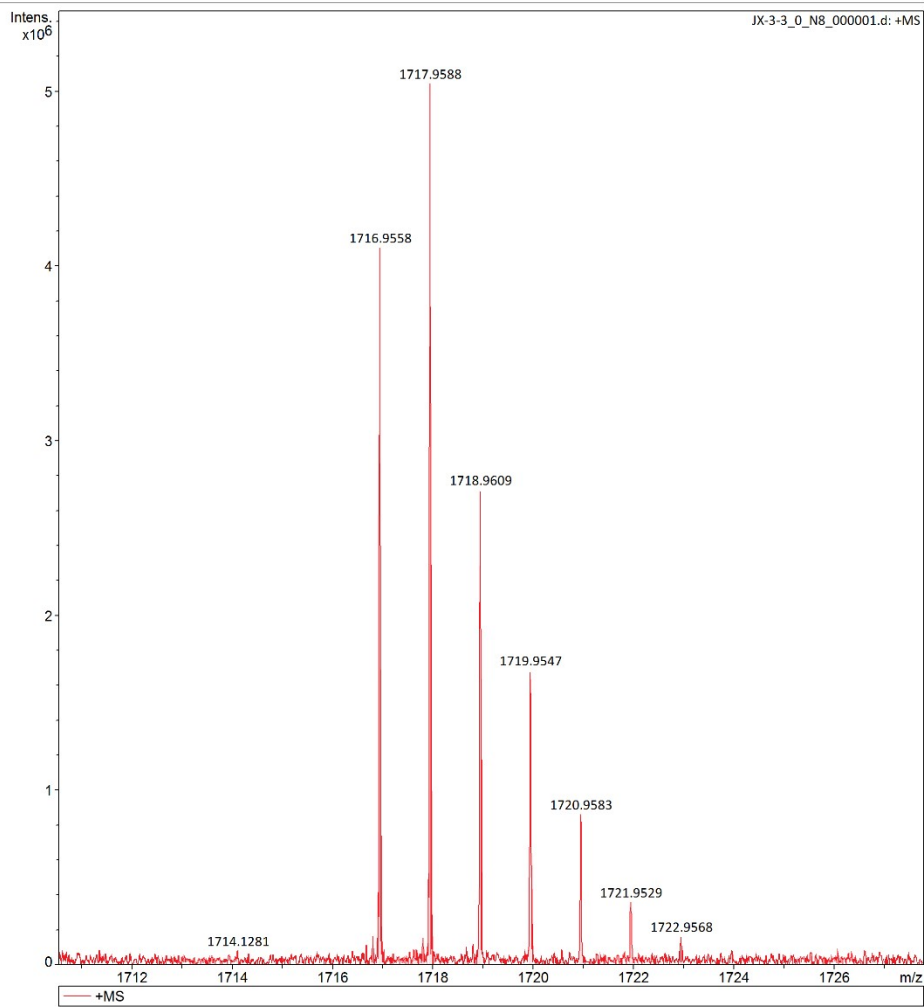


Figure S27. MS of compound 8.

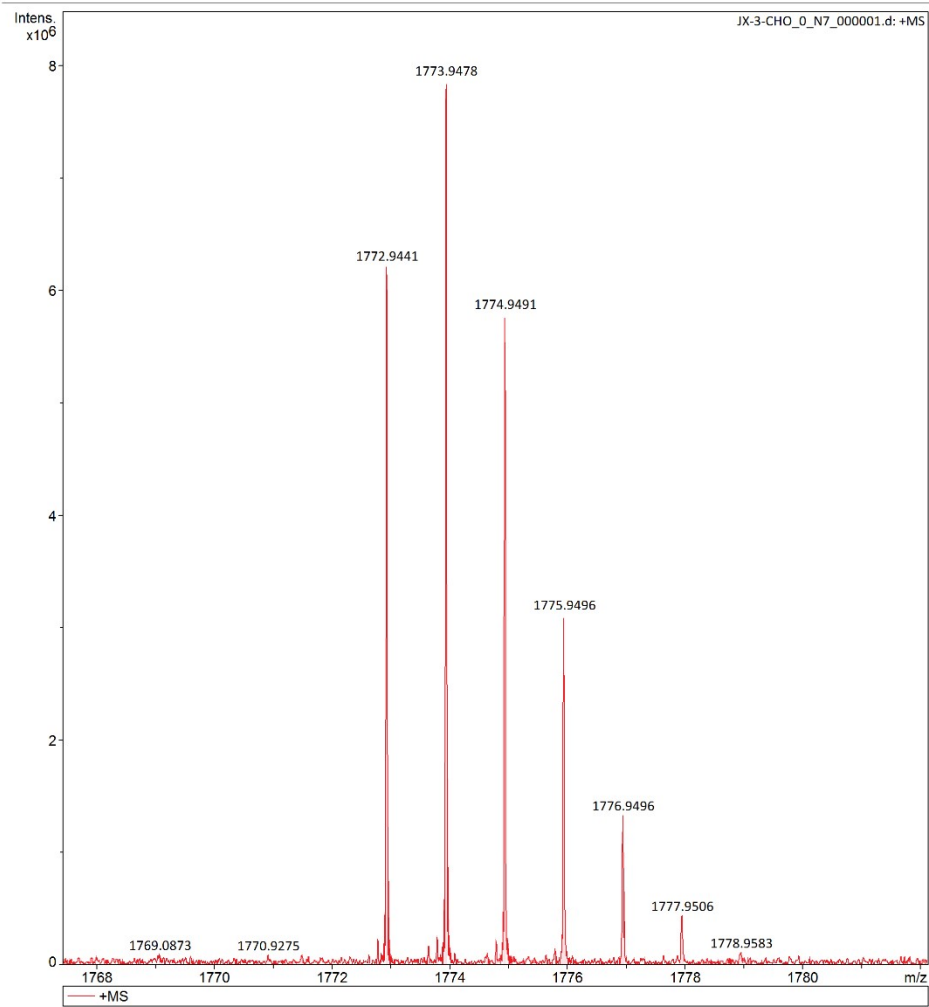


Figure S29. MS of compound 9.

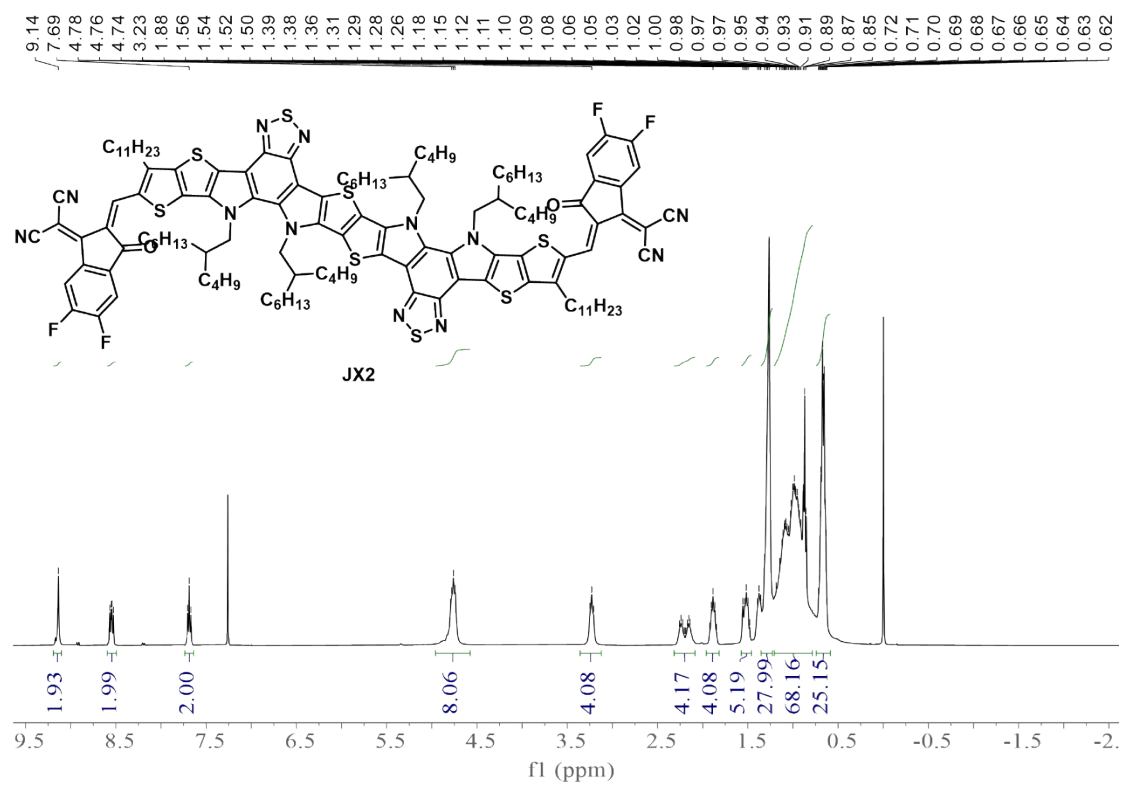


Figure S30. ¹H NMR spectrum of JX2 at 300 K in CDCl₃.

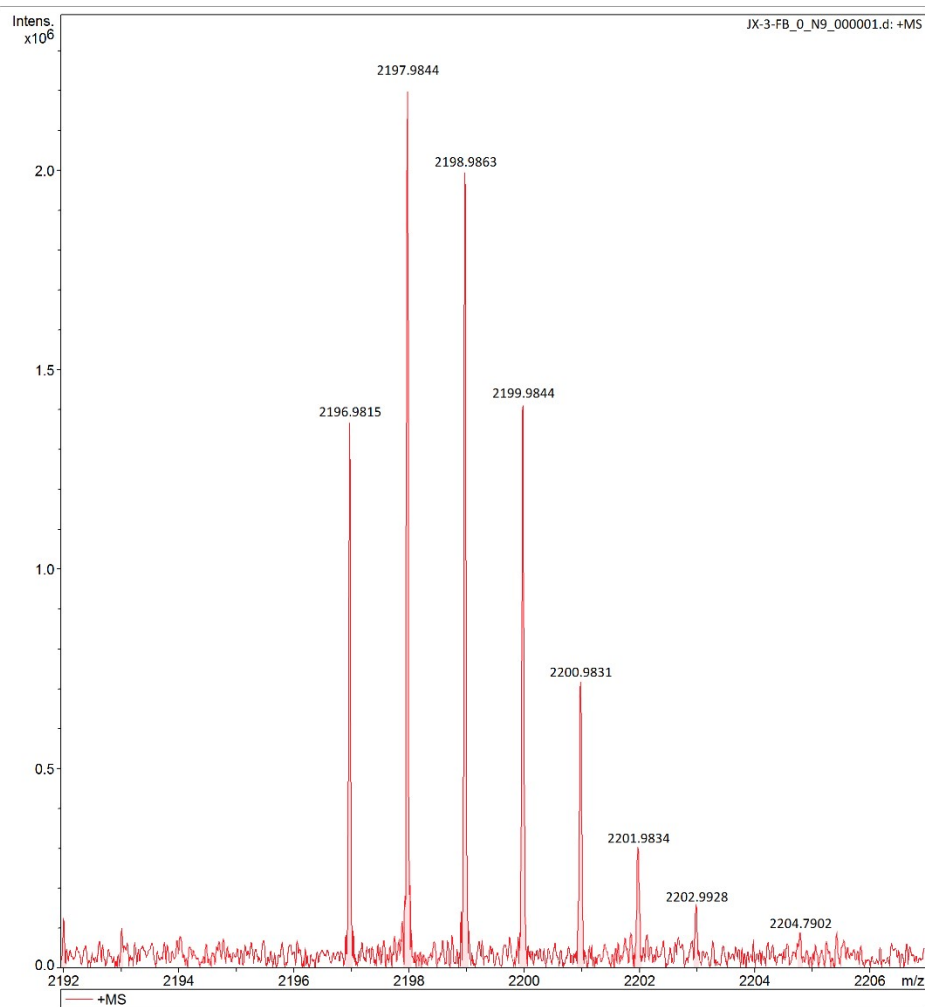


Figure S31. MS of JX2.

4. Note S1.

Computational methods in this work. All the alkyl chains of the starting single molecules were replaced with methyl groups (-CH₃) to reduce the computational requirements. The structures were subsequently optimized with Density Functional Theory (DFT) in vacuum within the Gaussian 16 software. The structure optimization, frequency analysis, energy level of frontier molecular orbital, and the reorganization energy were obtained at the Becke three-parameter Lee-Yang-Parr (B3LYP)² hybrid functional with the 6-31G(d) basis set³.

Theoretical density distribution ΔQ : ($\Delta Q = \Psi^2_{\text{LUMO}} - \Psi^2_{\text{HOMO}}$) is along the longest axis (backbone) of the defined molecules.⁴

The calculation method of E_{loss} . the total E_{loss} can be calculated by the equation:

$$E_{\text{loss}} = E_g - qV_{OC}$$

Where E_g can be calculated by the crossing point of normalized absorption and photoluminescence spectra.

The detailed components of E_{loss} can be categorized into three parts based on the Shockley-Queisser (SQ) limit⁵⁻⁷:

$$E_{\text{loss}} = \Delta E_1 + \Delta E_2 + \Delta E_3 = (E_g - qqV_{OC}^{SQ}) + (qV_{OC}^{SQ} - qV_{OC}^{rad}) + (qV_{OC}^{rad} - qV_{OC})$$

Where $V_{OC}^{SQ} = \frac{kT}{q} \ln \left(\frac{J_{SC}^{SQ}}{J_0^{SQ}} + 1 \right) \cong \frac{kT}{q} \ln \left(\frac{q \cdot \int_{E_g}^{+\infty} \Phi_{AM1.5G}(E) dE}{q \cdot \int_{E_g}^{+\infty} \Phi_{BB}(E) dE} \right)$, $\Phi_{BB}(E)$ is black body emission at

room temperature. Thus, for the unavoidable $\Phi_{BB}(E)$ radiative recombination ΔE_1 :

$$V_{OC}^{rad} = \frac{k_B T}{q} \ln\left(\frac{J_{SC}}{J_{0,rad}} + 1\right) \cong \frac{kT}{q} \ln\left(\frac{q \cdot \int_{E_g}^{+\infty} \Phi_{AM1.5G}(E) dE}{q \cdot \int_{E_g}^{+\infty} \Phi_{BB}(E) dE}\right)$$

Thus, for the radiative recombination ΔE_2

$$\Delta E_2 = qV_{OC}^{SQ} - qV_{OC}^{rad}$$

Finally, for the non-radiative recombination loss ΔE_3

$$\Delta E_3 = qV_{OC}^{rad} - qV_{OC}$$

Where V_{OC} is the open circuit voltage of the OSC.

5. Tables S1-S7.

Table S1. The optical and electrochemical data of NFAs in this work.

Comp	^a $\lambda_{\max}^{\text{sol}}$ (nm)	$\lambda_{\max}^{\text{film}}$ (nm)	$\lambda_{\text{edg}}^{\text{film}}$ (nm)	^b $E_{\text{g}}^{\text{onset}}$ (eV)	^c HOMO (eV)	^c LUMO (eV)
JX1	742	786	886	1.39	-5.41	-3.77
JX2	759	829	966	1.28	-5.33	-3.79

^a $\lambda_{\max}^{\text{sol}}$ was obtained from UV-*Vis* absorption spectra of JX2 in chloroform solution. ^bOptical band gap ($E_{\text{g}}^{\text{onset}}$) was calculated by $1240/\lambda_{\text{edg}}^{\text{film}}$. ^cThe highest occupied molecular orbital (HOMO) and lowest unoccupied molecular orbital (LUMO) energy levels were calculated from the onset oxidation potential and the onset reduction potential in Supplementary Figure S2, using the equation $E_{\text{HOMO}} = -(4.80 + E_{\text{ox}}^{\text{onset}})$ eV, $E_{\text{LUMO}} = -(4.80 + E_{\text{re}}^{\text{onset}})$ eV.

Table S2. Detailed photovoltaic parameters of the PCE10:JX1 based devices processed by varied conditions under illumination of AM 1.5 G, 100 mW/cm².^a

D/A [w/w]	DIO [v/v]	TA[°C]	V_{oc} [V]	J_{sc} [mA cm ⁻²]	FF [%]	PCE [%]
1:1	-	90	0.781	11.46	37.04	3.32
1:1.2	-	90	0.798	14.26	39.01	4.42
1:1.4	-	90	0.789	14.41	39.43	4.46

^aThe device architecture is ITO/PEDOT:PSS/active layer/PNDIT-F3N/Ag; D=6 mg/mL in chloroform; the resulting solutions were spin-casted at 2000 rpm for 30 s onto the PEDOT:PSS layer.

Table S3. Detailed photovoltaic parameters of the PCE10:JX2 based devices processed by varied conditions under illumination of AM 1.5 G, 100 mW/cm².^a

D/A [w/w]	DIO [v/v]	TA [°C]	V _{oc} [V]	J _{sc} [mA cm ⁻²]	FF [%]	PCE [%]
1:1	-	90	0.803	18.88	59.29	9.12
1:1.2	-	90	0.801	19.27	59.53	9.78
1:1.4	-	90	0.805	19.76	63.73	10.26
1:1.6	-	90	0.806	19.72	63.54	10.09
	-	80	0.796	19.72	65.16	10.14
	-	90	0.798	20.17	65.07	10.37
	-	100	0.797	19.74	65.64	10.22
1:1.4	0.25%	90	0.761	20.01	67.34	10.12
	0.30%	90	0.757	20.57	67.84	10.43
	0.35%	90	0.759	20.11	69.56	10.83
	0.40%	90	0.755	19.52	69.37	10.08

^aThe device architecture is ITO/PEDOT:PSS/active layer/PNDIT-F3N/Ag; D=6 mg/mL in chloroform; the resulting solutions were spin-casted at 2000 rpm for 30 s onto the PEDOT:PSS layer.

Table S4. Total energy loss values and different contributions in solar cells based on the SQ limit theory for optimized OSCs.

Active layer	E_g^a (eV)	$V_{OC, SQ}^b$ (V)	ΔE_1^c (eV)	$V_{OC, rad}^b$ (V)	ΔE_2^d (eV)	ΔE_3^e (eV)	ΔE_3^f (eV)	V_{OC} (V)	E_{loss}^g (eV)
PCE10:JX1	1.497	1.226	0.271	1.065	0.161	0.268	0.302	0.797	0.700
PCE10:JX2	1.326	1.069	0.257	0.984	0.085	0.225	0.261	0.759	0.567

[a] E_g is estimated on the basis of the derivatives of the EQE spectra ($dEQE/dE$, black curves)

(Figure S11). [b] V_{OC}^{SQ} is the upper limit for the V_{OC} of the solar cell derived in the Shockley-Queessier

theory. V_{OC}^{rad} is the radiative recombination limit for the V_{OC} of the solar cell, which can be

$$V_{OC}^{SQ} = \frac{kT}{q} \ln \left(\frac{J_{SC}^{SQ}}{J_0^{SQ}} + 1 \right) \cong \frac{kT}{q} \ln \left(\frac{q \cdot \int_{E_g}^{+\infty} \phi_{AM1.5G}(E) dE}{q \cdot \int_{E_g}^{+\infty} \phi_{BB}(E) dE} \right). \quad [c]$$

determined by the equation:

$$\Delta E_1 = E_g - qV_{OC}^{SQ}; \quad [d] \quad \Delta E_2 = qV_{OC}^{SQ} - qV_{OC}^{rad}; \quad J_{0,rad} = q \int EQE(E) \phi_{BB}(E) dE;$$

$$V_{OC}^{rad} = \frac{k_B T}{q} \ln \left(\frac{J_{SC}}{J_{0,rad}} + 1 \right). \quad [e] \quad \Delta E_3 = qV_{OC}^{rad} - qV_{OC}. \quad [f] \quad \Delta E_3 \text{ is calculated from the } EQE_{EL}, \text{ through the}$$

equation of $\Delta E_3 = -kT \ln(EQE_{EL})$ [V]. [g] $E_{loss} = \Delta E_1 + \Delta E_2 + \Delta E_3$.

Table S5. Detailed photovoltaic parameters of the PCE10:JX1 based devices by optimal conditions under illumination of AM 1.5 G, 100 mW/cm².^a

Active layer	V_{oc} [V]	J_{sc} [mA cm ⁻²]	FF [%]	PCE [%]
PCE10:JX1	0.801	17.93	46.89	6.63
	0.788	16.98	43.35	5.71
	0.795	17.18	43.08	5.79
	0.794	17.23	43.92	5.91
	0.789	17.01	43.73	5.77
	0.799	17.43	45.50	6.23
	0.797	17.46	45.61	6.24
	0.796	17.21	45.54	6.14
	0.793	17.42	45.48	6.18
	0.792	17.46	45.90	6.24
Average ^b	0.794	17.33	44.90	6.08

^aThe device architecture is ITO/PEDOT:PSS/active layer/PNDIT-F3N/Ag; D=6 mg/mL in chloroform with 0.35 vol% DIO; the resulting solutions were spin-casted at 2000 rpm for 30 s onto the PEDOT:PSS layer; TA (90 °C). ^bThe average values are obtained from 10 devices.

Table S6. Detailed photovoltaic parameters of the PCE10:JX2 based devices by optimal conditions under illumination of AM 1.5 G, 100 mW/cm².^a

Active layer	V_{OC} (V)	J_{SC} (mA cm ⁻²)	FF (%)	PCE (%)
PCE10:JX2	0.761	19.98	69.59	10.75
	0.759	20.19	69.56	10.83
	0.757	20.18	69.56	10.81
	0.759	20.01	69.37	10.72
	0.757	19.93	69.02	10.58
	0.753	19.90	69.65	10.61
	0.755	19.96	68.94	10.56
	0.761	20.39	69.70	10.99
	0.756	19.95	69.59	10.67
	0.758	20.28	68.46	10.70
Average ^b	0.758	20.08	69.35	10.72

^aThe device architecture is ITO/PEDOT:PSS/active layer/PNDIT-F3N/Ag; D=6 mg/mL in chloroform with 0.35 vol% DIO; 2000 rpm for 30 s; TA (90 °C). ^bThe average values are obtained from 10 devices.

Table S7. Crystal parameters extracted from GIWAXS.

film	q (010, Å ⁻¹)	d-space ^a (010, Å)	FWHM (010, Å ⁻¹)	CCL ^b (010, Å)	q (100, Å ⁻¹)	d- space ^a (100, Å)	FWHM (100, Å ⁻¹)	CCL ^b (100, Å)
JX1	1.630	3.85	0.587	9.63	0.378	16.61	0.538	10.51
JX2	1.660	3.78	0.551	10.26	0.447	14.05	0.383	14.76
PCE10:JX1	1.635	3.84	0.731	7.73	0.428	14.67	0.831	6.80
PCE10:JX2	1.659	3.79	0.584	9.68	0.433	14.50	0.206	27.44

^aCalculated from the equation: d-spacing = $2\pi/q$. ^bObtained from the Scherrer equation: CCL = $2\pi K/FWHM$, where FWHM is the full-width at half-maximum and K is a shape factor (K = 0.9 here).

6. References.

1. P. K. Madathil, S. Cho, S. Choi, T.-D. Kim and K.-S. Lee, *Macromolecular Research*, 2018, **26**, 934-941.
2. A. D. Becke, *The Journal of Chemical Physics*, 1993, **98**, 5648-5652.
3. P. C. Hariharan and J. A. Pople, *Mol. Phys.*, 1974, **27**, 209-214.
4. X. Wan, C. Li, M. Zhang and Y. Chen, *Chem. Soc. Rev.*, 2020, **49**, 2828-2842.
5. M. Gruber, J. Wagner, K. Klein, U. Hörmann, A. Opitz, M. Stutzmann and W. Brütting, *Adv. Energy. Mater.*, 2012, **2**, 1100-1108.
6. U. Rau, B. Blank, T. C. M. Muller and T. Kirchartz, *Phys. Rev. Appl.*, 2017, **7**, 044016.
7. Y. Wang, D. Qian, Y. Cui, H. Zhang, J. Hou, K. Vandewal, T. Kirchartz and F. Gao, *Adv. Energy. Mater.*, 2018, **8**, 1801352.